ACS APPLIED ELECTRONIC MATERIALS

pubs.acs.org/acsaelm Review

Convergence of Implantable Bioelectronics and Brain–Computer Interfaces

Minh Anh Huynh, Thanh-Ha Nguyen, Tuan-Khoa Nguyen,* and Nam-Trung Nguyen*

Cite This: https://doi.org/10.1021/acsaelm.3c00879 Read Online

ACCESS | Metrics & More | Article Recommendations

ABSTRACT: Missing neuronal communication between parts of the body and the brain can cause organ failures or life-threatening conditions including cardiovascular and neurological diseases. The implantable brain–computer interface (BCI) is an emerging interdisciplinary technology that can bridge the communication gap, restoring organ functions and treating neurological disorders. Since the success of the first battery-powered pacemaker in 1958, bioelectronics technology has made a prodigious leap toward a wide range of biomedical applications such as therapeutics, diagnostics, and assistive organ implants. The latest developments in material sciences and device integrations have enabled a technological paradigm shift from rigid to soft and mechanically conformal implantable BCI devices that could eliminate device–tissue mismatches. However, achieving mechanical and electrical stability with organic- and nanomaterial-based electronics implanted in the body is a big challenge. Recent advances in inorganic and wide bandgap materials for BCI devices provide a promising route to solve this bottleneck due to their stability, modalities, and standardized manufacturing processes. Nevertheless, several remaining key obstacles still hinder the applications of soft BCI devices. This review summarizes the latest developments and key challenges of this emerging field, focusing on technological and scientific aspects such as materials, device structures, modulation, sensing, power, and communication. Current challenges and future perspectives of this emerging technology will also be discussed.

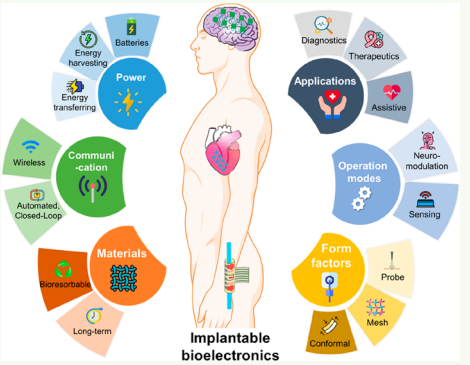

KEYWORDS: *bioelectronics, brain–computer interface, flexible electronics, implanted electrode, implantable electronics, neuromodulation*

1. INTRODUCTION

Neurological activities are vital for the body to maintain its complex functions. For instance, as the central commanding computer, the brain regulates cardiac functions via the vagus nerve,[1] as well as arm and leg movements via peripheral nerves.[2] Any communication disruption between the brain and nerves can cause severe cardiovascular diseases (i.e., cardiac arrest, myocardial infarction, stroke)[3] and neurological and motor disorders (i.e., Parkinson's disease, epilepsy).[4] Brain–computer interfaces are a class of computer-based, medical devices that can bypass normal communication pathways between the brain and peripheral nerves to regulate dysfunctional nerves.[5] A typical BCI device comprises (i) upstream electrodes and (ii) an analog-to-digital converter (ADC) and a digital-to-analog converter (DAC), as well as (iii) downstream electrodes. Upstream electrodes collect analog electrical signals from the brain, then transmit to the ADC that translates analog signal to digital signal. The digital signal is processed and translated back to an analog signal through the DAC. The analog electric signals are then transmitted to the downstream electrodes to stimulate dysfunctional nerves and restore their normal activities. The term BCI shares similarities with other terms such as brain–machine interface (BMI),[6−9] mind–machine interface (MMI),[10−13] and neural interface (NI).[14−19] Since the first report in the 1970s,[20] BCI technology has advanced with biomedical applications of implantable devices. Common BCI devices fall into two main categories: wearable (noninvasive) and implantable (invasive) devices. Wearable BCI have been dominantly developed in the early stage of the technology. This is attributed to the fact that wearable devices are easy to deploy and disassemble. The devices have minimal side effects to the wearer. However, the intrinsic features of wearable BCI devices only permit them to serve as monitoring tools for certain health signals through the skin with limited therapeutic functions. In contrast, implantable BCI devices come directly in contact with internal tissues. Thus, a vast range of therapeutics can be implemented. For example, deep brain stimulators (DBS) and cardioverter defibrillators are among the most common implanted BCI devices with a range

Received: July 17, 2023
Revised: October 6, 2023
Accepted: October 8, 2023

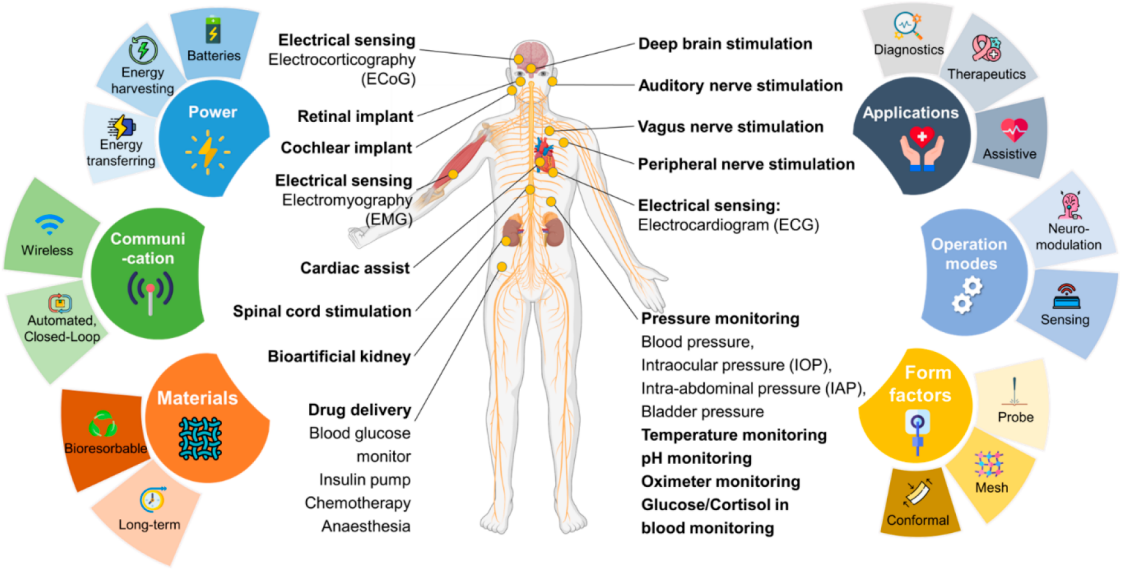

Figure 1. Representative mainstream applications of implantable BCI devices in therapeutics and diagnostics with key considerations of electrode form factors, materials, modulation, power, and communication. All images and icons from refs 79 and 80 with permissions.

of commercially available products. Furthermore, implanted BCI can yield a reliable and high signal-to-noise ratio (SNR)[21,22] for vital signals for precision disease detection and prevention as compared to wearable devices or hospital-based diagnostic tools.

Figure 1 summarizes mainstream applications and technical requirements for current implantable BCI devices. The most prominent application areas of implantable BCI include the vagus nerve,[1,23−27] sacral nerve,[28,29] spinal cord,[30−35] deep brain stimulation[20,36−42] for treatment of organ dysfunctions,[43−47] and cochlear[48−51] and retinal implants[52−57] for recovery of lost senses. Damages from accidents disrupt the transmission of electrical signals from the brain to the peripheral nerve that regulates muscle contraction. This results in temporary or permanent losses of motor functions and disability. Nevertheless, implantable BCI can bypass this disconnection by collecting and transmitting control signals from the brain to stimulate motor nerves. As such, electrical stimulation schemes can restore lost neural signals regulating auditory, vagus, and nerves functions. Habibagahi et al. introduced an implanted device with a wirelessly powered miniaturized BCI device for vagus nerve stimulation (VNS). This was the first demonstration of a wireless and batteryless VNS with more than 5 cm operation range.[25] Cuttaz et al. implemented a stretchable, fully polymeric electrode array with a width of 2 mm that was implanted and tested for peripheral nerve stimulation.[58] Woodington et al. reported a thin, flexible device with a gold electrode 20 mm in length and 5 mm in width with integrated microchannels. The device was validated in vitro and on human cadaver models for minimally invasive spinal cord stimulation (SCS).[30] Corridion et al. surveyed studies on bioartificial kidneys and their potential to support kidney function for people with a kidney disease.[43] Implantable BCI can also monitor body vital signs. Liu et al. reported an in vivo 16-channel recording using mesh syringe electronics injected into a mouse brain for monitoring electrocorticography (ECoG).[60] For nerve stimulation, Cuttaz et al. introduced a fully polymeric stretchable electrode array for peripheral nerve stimulation. Due to its flexibility, the 90-μm polymeric electrode arrays curl in and embrace and electrically stimulate the nerve.[58] Furthermore, Woodington et al. developed a 5 mm-wide flexible device that can roll up into the shape of a standard transdermal probe. The team implanted the device at the site of interest before unfolding it into its paddle shape and subsequently electrically stimulating the spinal cord.[30] The team utilized photolithography and soft lithography to fabricate a thin, flexible device with gold electrodes and integrated microchannels for minimally invasive spinal cord stimulation.

Losses of vision and hearing can be restored by neural stimulation of neural retinal or auditory nerves. For example, Eggenberger's team developed the passive laser-micromachined Phoenix99 Bionic Eye which was implanted into an ovine eye model and lasted for up to 100 days. The bionic eyes converted visual signals into electric signals that were then delivered to the retinal tissue to restored vision. The fully implantable system incorporated a visual stimulator connected to a behind-the-ear telemetry implant via a flexible cable. The stimulator was packed in an extraocular hermetic ceramic/titanium capsule and connected to a suprachoroidal electrode array made of medical-grade silicone elastomer and platinum (Pt) for biostability and biocompatibility.[59] Deep et al. reported a fully implantable MEMS-based autonomous cochlear implant for stimulating the auditory nerve, assisting people with auditory nerve defects to improve their hearing.[61] The ear-worn microphone detects and converts sound into an electrical signal and sends it to an external sound processor, which delivers the encoded stimulating signal. The receiver-stimulator turns these digital signals into electrical pulses that are delivered to multiple electrodes implanted in the eardrum. The electrodes electrically stimulate the spiral ganglion cells and auditory axons, which subsequently send signals to the brain.

Taking advantage of recent advances in materials, integration, packaging, and communication technologies, efforts have been continuously devoted to developing the next generation of BCI implantable devices with added functions. The latest development in micro/nanotechnologies allow for the integration of electronic components with size ranging from micrometers to millimeters (i.e., transistors, microfluidics, and

https://doi.org/10.1021/acsaelm.3c00879
ACS Appl. Electron. Mater. XXXX, XXX, XXX−XXX

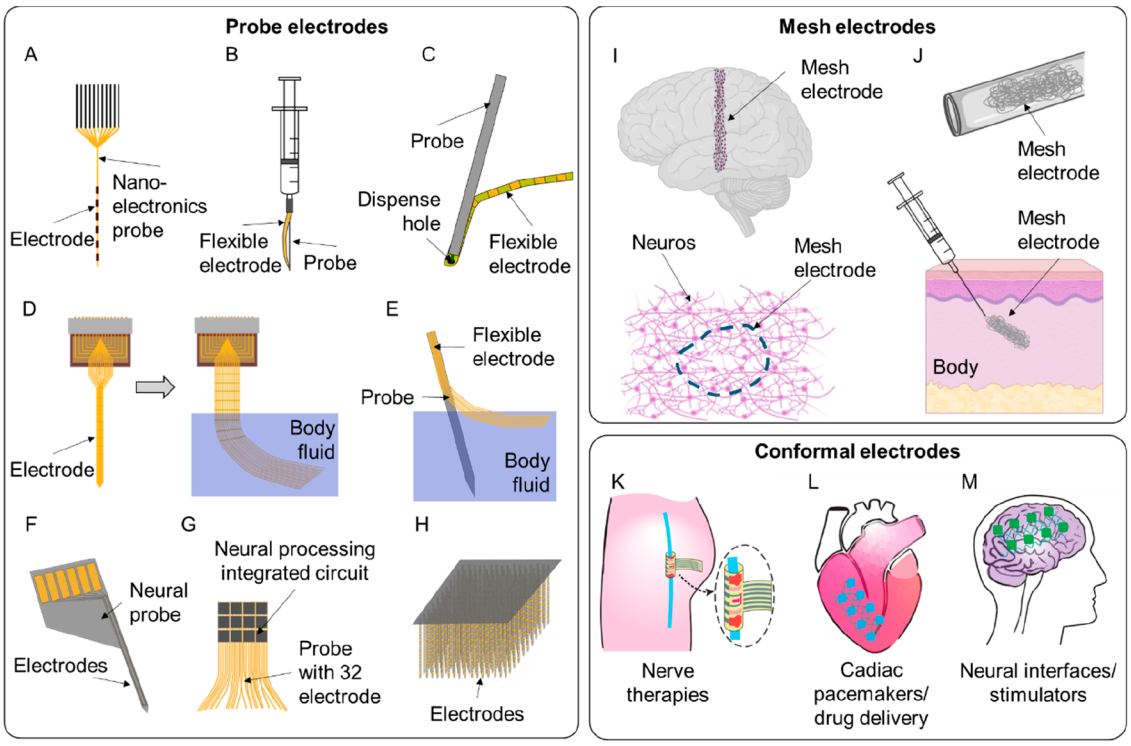

Figure 2. Form factors of BCI systems. Probe electrodes: (A) Ultraflexible nanoelectronics thread (NET-e) probe attaches electrodes with cross-sectional areas smaller than 10 μm^2. Redrawn from ref 88, with permission. (B) Flexible electrode connected to connector and attached a 20 mm sinusoidal probe to improvise insertion carrier for successful brain penetration and electrode insertion. Redrawn from ref 89, with permission. (C) Probe electrode combined with an auxiliary tool by a probe−hole structure. Redrawn from ref 90, with permission. (D) Neurotassel electrodes with a 12 mm wide and 3 mm high microelectrode filaments. Redrawn from ref 91, with permission. (E) The electrode combined with the auxiliary tool by a electrostatic adsorption. Redrawn from ref 92, with permission. (F) A parylene-C neural probe with six 40-μm diameter electrodes and PEDOT nanostructured and gold electrodes. Redrawn from ref 93, with permission. (G) High-throughput electrodes with more than 1000 channels. Redrawn from ref 7, with permission. (H) High-throughput and high-density 3D electrode array. Redrawn from ref 94, with permission. Mesh electrodes: (I) Mesh electrodes implanted in brain tissue and the interface between mesh electronics and the brain tissue. Redrawn from ref 95, with permission. (J) Syringe-injectable electrodes. Redrawn from ref 60, with permission. Conformal electrodes: (K) Flexible SiC/SiO_2 wrapped around a sciatic nerve. Redrawn from ref 97, with permission. (L) BCI for cardiac biophysical and biological sensing. Redrawn from refs 99 and 100, with permission. (M) Electrode arrays attached to the brain. Redrawn from ref 98, with permission.

optogenetics devices) along with electrode arrays for real-time monitoring during treatments. Therefore, integrated BCI sensing devices would enable in-body monitoring of vital signals for disease detection and prevention.[62] Common measurable electrical activities in the body include action potential,[63,64] electroencephalogram (EEG),[65] electromyography (EMG),[65] and electrocorticogram (ECoG)[66] to track brain, nerves, muscles, and cell activities. In addition, implantable sensors can monitor other vital physical signals such as temperature,[67,68] pressure,[69−71] and blood flow[72] to supplement the main monitoring functions.

There are several critical considerations for designing implantable therapeutic BCI devices. First, the evolution from rigid to soft implantable BCI platforms can seamlessly offer comfort to patients, minimizing foreign body responses and eliminating device damage from daily activities. Soft implanted electrodes minimize foreign body responses from the host organs while establishing minimal invasive tissue−machine interfaces. Second, while the overall footprint of BCI continues to shrink due to micro/nanotechnology, further efforts have been devoted toward high-density, large-area designs[73] for better scalability and functionality. Third, new material platforms and packaging schemes have been explored to enhance safety compliances and lifetime tuneability. While organic bioelectronic materials have emerged as a promising route to soft and mechanically conformal BCI devices,[74−77] their electrical and chemical stability in the body is still inadequate. These unmet requirements could be addressed by employing inorganic wide bandgap semiconductors,[78] but new engineering pathways are urgently needed to overcome the mismatch between their rigidity and the soft nature of tissue.

The present review summarizes recent progress in the aforementioned research directions. We focus on critical aspects of implantable BCI electrodes for medical and healthcare applications, such as device form factors, neuromodulation and sensing schemes, and bioresorbable versus long-term electrodes, as well as power and communication. This paper starts with an overview of mainstream applications of implantable BCI devices, followed by a survey on device form factors, neuromodulation and sensing schemes, materials for bioresorbable and long-term electrodes, and power and communication schemes. Finally, we conclude by offering insights into unresolved challenges and perspective of future research directions.

2. ELECTRODE FORM FACTORS

The geometry of BCI electrodes dictates how they physically interface with the targeted tissue, depending on therapeutic requirements. Probe electrodes are an important class of implantable BCI. The stiffness of the electrodes allows for their

https://doi.org/10.1021/acsaelm.3c00879
ACS Appl. Electron. Mater. XXXX, XXX, XXX−XXX

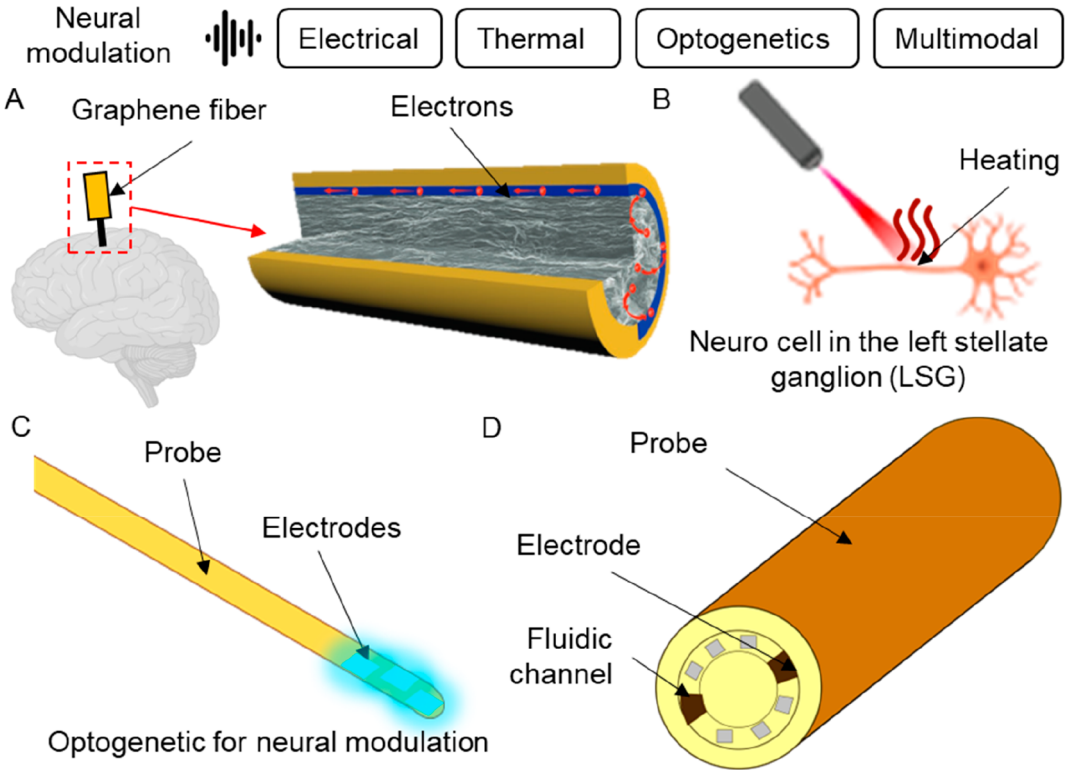

Figure 3. Neuromodulation modalities of BCI devices. Physical neural modulation: (A) Electrical neural modulation by an inserted microelectrode. Redrawn from ref 109, with permission. (B) Thermal neural modulation by polyethylene glycol−gold nanorods (PEG-AuNRs) photothermal neural inhibition. Redrawn from ref 111, with permission. (C) Optogenetic neural modulation by an optoelectronic probe with a Pt electrode. Redrawn from ref 112, with permission. Multimodal neural modulation: (D) Multifunctional flexible polymer fibers with an opto-electrophysiological mechanism for neural modulation. Redrawn from ref 101, with permission.

penetration into a tissue. Even though this type of BCI can enable broader access to tissue interface, they rely on using rigid probes[81−83] or other injection methods,[60,84] which complicates the implantation process and triggers foreign body responses. Conformal surface electrodes can overcome these limitations by providing minimally invasive large-surface-area contacts with tissue. This is attributed to the fact that these electrodes interface with the outermost layer of biological tissues, only possible with soft and conformal materials. This type of implantable BCI interface is important for delivering treatments on the organ surface and real-time large-area diagnostics. Recent advances in surface electrodes enables multiplexed mesh electronics with 3D integration that offer scalable, high-throughput interfaces for single-neuron recording.[85,86] However, the difficulties in deployment and unstable tissue contacts hinder the wider adoption of this unique electrode form factor.

Since the early stage of implantable BCI devices, rigid probe electrodes have been utilized.[87] Some examples of flexible systems with probe electrodes are a flexible nanoelectronic thread (NET-e) probe (Figure 2A),[88] a flexible electrode attached to a probe (Figure 2B),[89] an electrode connected with the auxiliary tool through a probe−hole structure (Figure 2C),[90] neurotassel electrodes with microelectrode filaments (Figure 2D),[91] an electrode combined with the auxiliary tool by an electrostatic adsorption (Figure 2E),[92] a parylene-C neural probe with six poly(3,4-ethylenedioxythiophene) (PEDOT) nanostructured and gold electrodes (Figure 2F),[93] high-throughput electrodes with more than 1000 channels (Figure 2G),[7] and a high-throughput and high-density 3D electrode array (Figure 2H).[94]

First, these electrodes can contact tissue in a 3D space that increases their efficacy. Second, the stiff construction of probe electrodes makes sensing and stimulating functions more stable than softer constructions. Third, probe electrodes are easier to position on cell-sized targets, making grafting and adjustment more accessible and faster than soft electrodes. However, probe electrodes damage tissues, leading to bleeding and discomfort. Additionally, due to their rigidity, only certain body parts can use probe electrodes. For instance, they only work in specific areas of the brain for sensing and stimulating internal organs.

Mesh electrodes have been serving as brain implants (Figure 2I)[95] and syringe-injectable electrodes (Figure 2J).[60] Mesh electrodes minimize damage to tissues due to its soft nature.[96] Moreover, implanting mesh electrodes into the body is more accessible due to its soft nature, allowing its injection into the subcutaneous layer. Mesh electrodes can attach to intricately structured internal organs to sense and stimulate. These tasks are not possible with probe electrodes. However, the drawbacks of mesh electrodes are the complex manufacturing process and difficult maintenance. Sometimes, it is more challenging to position the mesh electrodes than probe electrodes because due to the softness they are structurally unstable.

Conformal electrodes are a new emerging large-area, multifunctional counterpart of probe electrodes. This class of BCI electrodes utilizing soft materials enables unprecedented applications such as shape-changing BCI via microfluidic

https://doi.org/10.1021/acsaelm.3c00879
ACS Appl. Electron. Mater. XXXX, XXX, XXX−XXX

actuations to wrap around nerves (Figure 2K)[97] and flexible electrodes that can match the curvature of the brain surface (Figure 2L).[98] First, conformal electrodes are more suitable to deploy around cylindrical shapes such as nerves or muscle strings, which is more challenging for other electrode types. Second, they are capable of creating large comformal interface surfaces with neural tissues (e.g., brain, heart) thanks to the designed shape-shifting mechanisms. Compared to probe electrodes, conformal electrodes are typically softer and can limit side-effect injury to targeted tissues. As a major trade-off, the design and manufacturing of conformal electrodes are complex, especially for shape-changing structures. In addition, finding the right materials that are easy to change shape and chemically resistant but do not cause allergies or body rejection is not straightforward and requires further research.

3. BRAIN−COMPUTER INTERFACE FOR MODULATION AND SENSING

3.1. Modulation. Implantable BCI devices stimulate nerves and cells through neuromodulation schemes such as electrical, thermal, and optogenetics methods, which are physical. To deliver more complex therapeutic and diagnostic functions, multimodal neuromodulation should employ both physical and pharmacological stimuli.[101]

Electrical stimulation is most common for neural modulations for nerve stimulation,[18,102,103] deep brain stimulation (DBS),[36,104] and VNS.[105,106] Electric currents with tunable amplitudes, frequencies, and frequency bandwidths evoke responses when applied to the targeted tissues. The parameters for stimulating electrical signals vary across applications, but generally, short pulse durations in the range of microseconds (μs) are commonly used to minimize tissue damages.[44] A key metric for stimulation BCI electrodes is the charge injection capacity (CIC), where the maximum deliverable charge is measured against the corresponding unit area. The CIC range for a specific material class can vary from relatively low values (<0.5 mC/cm^2)[107] for noble metals (i.e., Au, Pt, Pd, Ir) to moderate values (1−5 mC/cm^2) for ceramics (e.g., iridium oxide (IrO_x) and titanium nitride) and conductive polymers (e.g., (poly(3,4-ethylene dioxythiophene):poly-(styrenesulfonate) (PEDOT:PSS)).[108] For example, Wang et al. developed flexible and free-standing microelectrode arrays based on graphene fiber for electrical modulation. A thin platinum coating worked as a current collector in a structure with low impedance and tremendous electrochemical properties. The research team implanted microelectrodes in a rat cerebral cortex and detected neuronal activity with an extremely high signal-to-noise ratio (SNR) of 9.2 dB in a surface with an area as small as an individual neuron. The apparent diameter (the diameter of a circle with a diameter equal to the longest width of the irregular fiber) of the microfibers was controlled, ranging from 20 ± 3 to 40 ± 5 μm. Researchers applied a thin coating of Pt (in the range of 200 nm) as the current collector on the wet-spun graphene microfibers. The lengths of the microfibers increased from ≈0.5 to 5 cm (Figure 3A).[109] The electrical stimulation method has the advantage of a fast response time (∼400 ms).[110] This method has the disadvantage that it can affect the patient's tissue because the electric current spreads to the tissue adjacent to the nerve or stimulated cells. In addition, if the device's insulation is not good or leaks, the current can also affect the cells around the device.

Ye et al. conducted thermal neural modulation using polyethylene glycol−gold nanorods (PEG-AuNRs) with near-infrared (NIR)-sensitive gold nanorods (AuNRs). AuNRs are precisely regulated and applied to inhibit LSG function and neural activity, leading to ameliorating myocardial ischemia-induced ventricular arrhythmias (VAs) in a canine model. Specifically, the optimized AuNRs are synthesized and injected into the left stellate ganglion (LSG) of anesthetized dogs, then followed by 5 min of NIR laser irradiation at a wavelength of 808 nm (Figure 3B). The thermal neural modulation method has the advantage that the effect on cells is less than electrical modulation because the highest temperature of the modulation is 65 °C. This thermal-based method required long stimulation times due to the slow thermal response for the stimulated cell or nerve to reach the desired temperature (e.g., 270 s to heat from 35 to 65 °C).[111] In addition, the fabrication of the device and the modulation method with a high accuracy are more complex than other methods due to the small cell size and the limitation of the fabrication method.

Wu et al. introduced monolithically implanted microscopic light emitting diodes (mLEDs) for optogenetic neural modulation. Each mLED and recording site has the same dimensions as a pyramidal neuron soma, providing confined emission and electrophysiological recording of action potentials and local field activity. The four-shank probe integrated with 12 mLEDs and 32 recording sites, into the CA1 pyramidal layer of anesthetized and freely moving mice (Figure 3C).[112] The optogenetic neural modulation method has the advantage of a faster heating time to the desired temperature to stimulate the cells than thermal modulation. It takes 10 s to heat from 37 °C to over 43 °C.[112] It has the limitation that arranging the mLEDs into the microphone probe will be difficult due to limited space. In addition, it requires a complex control system to control the mLEDs accurately and reliably. The optogenetic neural modulation implantable BCI device is more complex, difficult to manufacture, and expensive.

Combining the aforementioned modulation schemes yields more complex therapeutic functionality and enhances treatment efficacy. Park et al. implemented probes that inject viral vectors carrying opsin genes, while concurrently providing collocated neural recording and optical stimulation. The miniature footprint (<200 μm) and modest weight (<0.5 g) of these probes allowed for multiple implantations into a mouse brain, which enable opto-electrophysiological investigation of projections from the basolateral amygdala to the medial prefrontal cortex and ventral hippocampus during behavioral experiments (Figure 3D).[101] This method has the advantage of combining many neural modulation methods to create the highest efficiency. This device can apply to many environments in the body, locations in the body, and different parts. However, it has the disadvantage that it will require a complex control system, and the manufacturing will also be more difficult, including manufacturing electrode microfluidic channels and combining them. Therefore, the cost of the device will also be higher than devices that only use one neural modulation method.

3.2. BCI Recording. Implantable BCI devices are capable of monitoring vital body parameters through sensing signal types such as biopotential, biochemical, and biophysical signals. First, biopotential signals include electrocardiogram (ECG or EKG), electroencephalogram (EEG), and electromyogram (EMG), representing the active state of the brain, body parts, and muscles. Second, molecular biochemicals,

https://doi.org/10.1021/acsaelm.3c00879
ACS Appl. Electron. Mater. XXXX, XXX, XXX−XXX

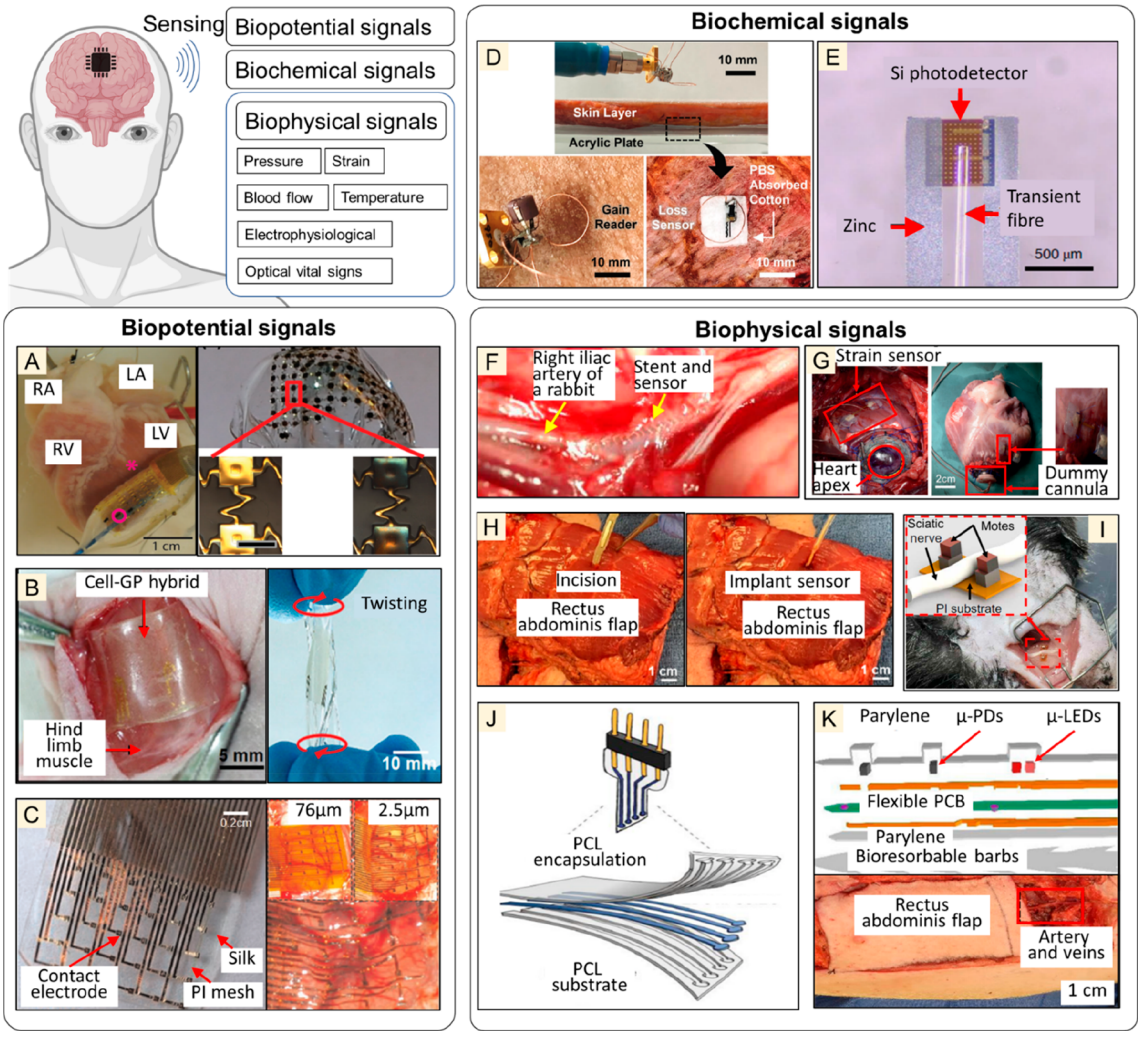

Figure 4. Types of sensing signals of BCI devices. Biopotential signals: (A) Electrocardiogram (ECG) monitor: Measurement by ECG flexible sensor. Reproduced with permission from ref 113. Copyright 2014, Wiley Online Library. (B) Electromyography (EMG) monitor: Measurement by implanted stretchable and transparent cell-sheet−graphene hybrid (Cell−GP hybrid) onto hind limb muscle of a nude mouse in vivo. Reproduced with permission from ref 114. Copyright 2016, Wiley Online Library. (C) Electrocorticography (ECoG) monitor: Electrode array (25-μm mesh) on a feline brain after dissolving the silk substrate. Reproduced with permission from ref 115. Copyright 2010, Nature Publishing Group. Biochemical signals: (D) Parity−time (PT) symmetric wireless biosensor detects tear glucose level for diabetes diagnosis and blood lactate level for lactic acidosis diagnosis. Reproduced with permission from ref 116. Copyright 2023, John Wiley & Sons, Ltd. (E) Bioresorbable Si photodetector with a bioresorbable fiber optic probe for spectroscopic characterization of biological tissues. Reproduced with permission from ref 117. Copyright 2019, Nature Publishing Group. Biophysical signals: (F) Pressure signal: Fully implantable, wireless vascular electronic system with printed sensors for wireless monitoring of hemodynamic. Reproduced with permission from ref 118. Copyright 2022, American Association for the Advancement of Science. (G) Strain signal: Fully implantable soft strain sensor for continuous heart volume monitoring. Reproduced with permission from ref 119. Copyright 2020, Wiley Online Library. (H) Blood flow: Implantable, wireless, self-fixing thermal sensors. Reproduced with permission from ref 72. Copyright 2022, Elsevier. (I) Temperature signal: Fully wireless temperature-sensing motes with ultrasound powering and data communication. Reproduced with permission from ref 67. Copyright 2021, American Association for the Advancement of Science. (J) Electrophysiological signal: All-polymeric transient neural probe for prolonged in vivo electrophysiological recordings. Reproduced with permission from ref 120. Copyright 2021, Elsevier. (K) Optical vital signal: Wireless, implantable near-infrared spectroscopic (NIRS) probing system for local-tissue oximetry. Reproduced with permission from ref 121. Copyright 2022, Nature Publishing Group.

including ions, analytes, and other biomarkers in the body, can be measured with implanted BCI chemical sensors. Third, biophysical signals include pressure and strain, temperature, viability, and electrophysiological signals from organs, blood vessels, and cells. These signals from implantable BCI devices are typically recorded in analog formats then transmitted to external modules via wire or wireless communications. Subsequently, the signals are converted from analog to digital forms then processed for data logging by externally integrated circuitries.

Biopotential. A variety of implantable BCI devices have been developed to detect biopotential signals such as action potential, ECG, EMG, and ECoG. Biopotential signals represent the action of neurons and muscles, generating signals with varying frequencies and amplitudes. Recording these biopotential signals allows for continuous monitoring abnormality in vital signals that can lead to organ failures. Chung et al. developed a flexible sensor implanted in a rabbit to monitor its ECG (Figure 4A).[113] Kim et al. implanted a stretchable and transparent cell-sheet−graphene hybrid (Cell−

https://doi.org/10.1021/acsaelm.3c00879
ACS Appl. Electron. Mater. XXXX, XXX, XXX−XXX

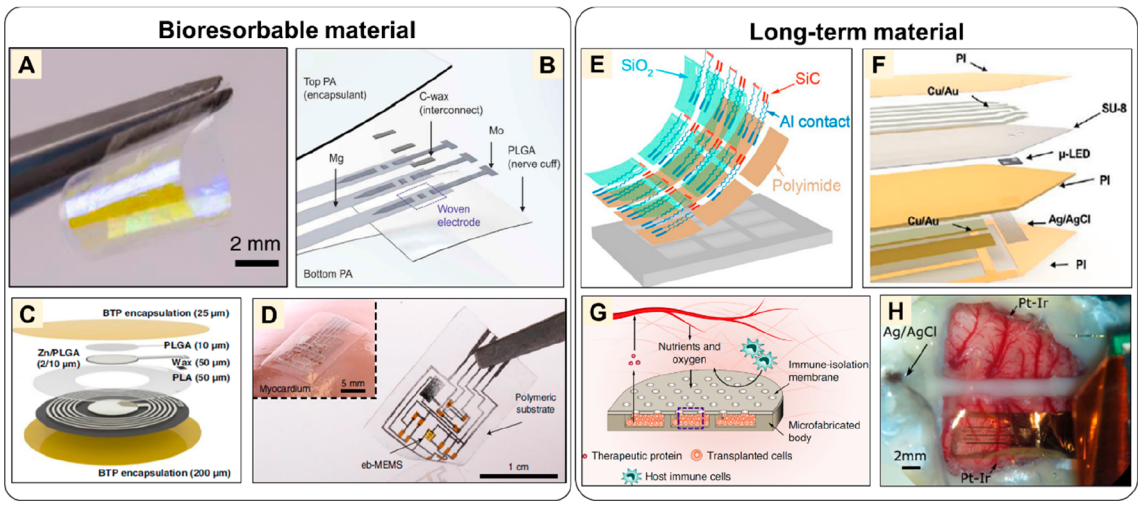

Figure 5. Materials for implantable BCI devices. Bioresorbable materials: (A) Bioresorbable optical filter based on a multilayer assembly of films of SiO_x and SiN_y. Reproduced with permission from ref 117. Copyright 2019, Nature Publishing Group. (B) Bioresorbable electrical stimulator for nerve conduction block consists of woven interconnects (Mg, Mo) and electrodes mounted on a nerve cuff (PLGA). Reproduced with permission from ref 124. Copyright 2022, American Association for the Advancement of Science. (C) Wireless, bioresorbable physiological biosensor with an inductor with thinned bottom electrode on a PLA substrate. Reproduced with permission from ref 125. Copyright 2022, Nature Publishing Group. (D) Flexible forms of ecoresorbable and bioresorbable MEMS (eb-MEMS) with a top structural polysilicon layer, an intermediate polysilicon layer, and a bottom silicon nitride insulating layer. Reproduced with permission from ref 126. Copyright 2022, Nature Publishing Group. Long-term materials: (E) Electronics device with a wide bandgap semiconductor nanomembranes SiC/SiO_2. Reproduced with permission from ref 97. Copyright 2020, John Wiley & Sons, Ltd. (F) Chemical sensor based on a polyimide substrate for long-term stimulating and monitoring in multiencephalic regions. Reproduced with permission from ref 128. Copyright 2020, Wiley Online Library. (G) Retrievable implant for the long-term encapsulation and survival of therapeutic xenogeneic cells with a polymeric membrane and a silicone body. Reproduced with permission from ref 132. Copyright 2020, Nature Publishing Group. (H) Graphene-active sensor arrays for chronic, wireless monitoring of wide frequency band epicortical neural activity. Reproduced with permission from ref 133. Copyright 2021, Nature Publishing Group.

GP hybrid) onto the hind limb muscle of a nude mouse to monitor EMG (Figure 4B).[114] Kim et al. implanted an electrode array (25-μm mesh) on a feline brain after dissolving the silk carrier substrate to monitor ECoG (Figure 4C).[115]

Biochemical. Efforts have been devoted to developing implantable BCI devices to monitor biochemical biomarkers and analytes presenting in blood or body fluids. For example, BCI devices can determine the glucose level for diagnosis and early treatment of diabetes. Takamatsu et al. developed a parity−time (PT) symmetric wireless biosensor that detects tear glucose levels for the diagnosis of diabetes and blood lactate levels for the diagnosis of lactic acidosis (Figure 4D).[116] In addition, detecting biomarkers and measuring their concentration allow for spectroscopic characterization of biological tissues. Bai et al. implemented a bioresorbable silicon photodetector with a bioresorbable fiber optic probe for spectroscopic characterization of biological tissues (Figure 4E).[117]

Biophysical. Implantable BCI devices are widely employed to sense biophysical signals for vital signs, including pressure sensor, and strain, temperature, humidity, electrophysiological, and optical sensors. These signals provide essential health parameters of a patient such as blood pressure, internal body temperature/humidity, and cell/tissue strain states. These parameters allow for assessing health condition, detecting abnormalities, and consequently providing timely and accurate treatment. Herbert et al. developed a fully implantable, wireless vascular electronic system with printed sensors for wireless monitoring of hemodynamics (Figure 4F).[118] Dual et al. reported a fully implantable soft strain sensor for continuously monitoring the heart volume (Figure 4G).[119] Lu et al. successfully demonstrated implantable, wireless, self-repairing thermal sensors to monitor microvascular blood flow in flaps and organ grafts (Figure 4H).[72] Shi et al. developed wireless temperature-sensing motes with powering through ultrasound and data communication to remotely monitor the temperature of a rat (Figure 4I).[67] Ferlauto et al. exploited an all-polymeric transient neural probe for prolonged in vivo electrophysiological recordings (Figure 4J).[120] Guo et al. acquired a wireless, implantable near-infrared spectroscopic (NIRS) probing system for monitoring local-tissue oximetry (Figure 4K).[121]

Long-term implantable BCI devices are now able to perform electrical and chemical sensing for long terms thanks to the use of materials that corrode slowly in the human body, and the solid and electrode surfaces are specially treated so electrical and chemical sensing can be performed up to weeks after surgery. Ling et al. implemented flexible electronics for monitoring in multiencephalic regions which can operate and monitor brain signals from a rat for a long period in a stable way. Four tentacle-like channels on the flexible electronics allow it to be implanted into several rat brain regions and deliver optical stimulation at particular wavelengths while keeping track of neural responses like action potentials and ionic concentrations. A μ-LED for optogenetic stimulation, four microelectrodes for biopotential monitoring and stimulation, and three ion-selective sensors that track Ca^{2+}, Na^+, and K^+ are all present on each channel's two stacked polyimide (PI) substrates. The μ-LED (190 μm× 110 μm× 8 μm) are coated with either phosphors or cadmium selenide (CdSe)/zinc sulfide (ZnS) quantum dots to provide different emission wavelengths. The μ-LED is enclosed by four microelectrodes (30 μm in diameter) made of Ti/Cu/Ti/Au multilayers that are parallel to one another. Gold nanoparticles (AuNPs) are applied to the surface to lower contact impedance during the

https://doi.org/10.1021/acsaelm.3c00879
ACS Appl. Electron. Mater. XXXX, XXX, XXX−XXX

measurement. Three working electrodes and one shared reference electrode are present in the three ion-selective sensors on the lower PI substrate. For ion-to-electron transduction, the working electrodes are modified with K^+/Na^+/Ca^{2+} selective membranes and covered with poly(3,4-ethylenedioxythiophene) polystyrenesulfonate (PEDOT:PSS). The reference electrode changed to reduce potential drift with a polyvinyl butyral (PVB) solid electrolyte and sodium chloride (NaCl). The resulting canal features an implantation-friendly sharp tip and total measurements of 600 μm × 2 cm × 80 μm. In order to provide programmable light stimulation and sensing, a wireless circuit synchronizes the working sequences of all channels and processes the associated signal. The wireless circuit can be easily placed into the skull, and all channels can be bent to adapt to implant placements with the least amount of brain damage. The complete system can remotely control and monitor neurological activity in freely moving animals without affecting their behaviors when fueled by a lithium-ion battery. Furthermore, post-treatment neural signals for the immunohistochemical analysis can be obtained 6 weeks after implantation surgery.[124]

4. MATERIALS FOR BIORESORBABLE AND LONG-TERM IMPLANTABLE BCI

4.1. Bioresorbable BCI Electrodes. Bioresorbable materials decompose and dissolve within a set period after the completion of the treatment task. Biodegradable implantable devices are frequently made of certain materials. Common possibilities for bioresorbable semiconductors include silicon, Ge, and ZnO. Mg, Mo, Zn, and W are the metals that provide useful biointerfaces and interconnects. Poly(lactic-*co*-glycolic acid) (PLGA) sheets are the soft substrate for bioresorbable devices. Silicon oxide (SiO_x) has frequently been employed as a temporary encapsulating layer for biodegradable electronics.[122] Bai et al. implemented a bioresorbable photonic device for spectroscopic characterization of physiological status and neural activity. The device can work for 45 days before becoming invisible under computed tomography, as evidence of complete bioresorption (Figure 5A).[117,123] Lee et al. developed electrodes that disintegrate into small pieces within two months and disappear completely at a moderate rate of 0.02 μm/day (Figure 5B), to prevent potential cytotoxicity to the bloodstream.[124] Bioresorbable materials have advantages of self-dissolving after a given period in operation. As such, subsequent removal surgeries are no longer required, reducing the patient recovery time and improving treatment efficacy. Moreover, these devices contribute to the protection of the environment. Yang et al. developed an eco-/bioresorbable form of MEMS using complementary metal−oxide semiconductor (CMOS) electronics, resistors, and capacitors, utilizing a multilayer structure of SiO_2/Si/SiO_2/W/SiO_2/SiN_x, doped monocrystalline silicon micromembranes (Si MMs), and a trilayer of Mo/SiO_2/W, without using plastic or other environmentally unfriendly materials following the decay (Figure 5C).[125] In addition, Yang et al. developed an eco-resorbable and bioresorbable microelectromechanical system, which can fully disassemble and dissolve just after 20 days (Figure 5D).[126] However, the weakness of bioresorbable materials is the unknown long-term health consequences of disintegrating in the body. These materials must undergo long-term testing and pass the rigorous checks of medical regulatory authorities. The compliance process will take time and money. Furthermore, implantable BCI devices made of these materials will not be suitable for long-term measurement as repeated surgery is expected for their delivery.

4.2. Long-Term BCI Electrodes. Long-term materials for implantable BCI devices can last for years or decades in the biophysical environment. The critical requirements for this class of BCI devices is the high resistance against chemical corrosion within the body, while maintaining electronics and electrical performance for sustaining continuous operations. Flexible implanted electronics require three essential elements to function sustainably: (i) a durable polymeric substrate to house electronic components, (ii) a long-term encapsulation layer for integrated circuits, and (iii) a reliable Faradaic interface for recording and stimulation. Due to its chemical inertness and thermal stability, polyimide is a typical soft substrate used to plan other electrical devices. Polymer substrates permanently anchor electronics. The deterioration of other integrated electronic components could be markedly slowed down by a SiO_x layer that is thick enough (e.g., 1 μm). Highly conductive metals like Ti and Au have been employed in several implanted devices.[122] Minev et al. designed and developed a soft neural interfaces implantable device that simulates the shape and mechanical behavior of the dura mater, the outermost layer that protects the brain and the spinal cord. The device consists of a transparent silicone substrate with a thickness of 120 μm, stretchable gold interconnects with a thickness of 35 nm, soft electrodes coated in a platinum−silicone composite with a diameter of 300 μm, and a compliant fluidic microchannel with a cross section of 100 μm × 50 μm. After 5 million electrical pulses, the platinum−silicone composite electrodes showed a substantial cathodal charge storage capacity of 46.9 ± 3.3 mC/cm^2 and a charge injection limit of 57 ± 9 μC/cm^2. The embedded electrodes survived cyclic deformation up to 20% strain over a million cycles, showing no change in impedance over time. In addition, the team tested these soft electrodes in four rats for 5 weeks. The impedance at 1 kHz remained consistent over this experiment. The outcomes demonstrate the long-term functionality, mechanical toughness, and electrochemical stability of this system.[127] Nguyen's team developed a sensor based on a wide bandgap material (i.e., silicon carbide (SiC)) that was estimated to last in the body for up to several decades with excellent stability (Figure 5E).[97] Ling et al. implemented flexible electronics for monitoring in multiencephalic regions which can operate and monitor brain signals from a rat for a long period in a stable way (Figure 5F).[128] Many research groups are developing long-term, flexible wide bandgap semiconductor devices. Phan et al. developed long-lived, transferred crystalline silicon carbide nanomembranes with thicknesses of 230 nm. After being soaked in 1× PBS for 12 days, there is no detectable non-Na^+ ion diffusion at a thickness of 50 nm for at least 60 days in PBS at 96 °C. These characteristics allow for multimodal temperature, strain, and other property sensing without additional encapsulating layers and Faradaic interfaces between active electronics and biological tissues.[129] Many microphone fabrication methods have been optimized and created to fabricate long-term flexible devices. Pham et al. created a sophisticated transfer printing technique based on sacrificial layer engineering for silicon carbide materials in stretchy electronic devices. The versatility of transferring complex microstructures from hard donor surfaces to flexible reception platforms is improved by using a sacrificial layer. Additionally, the sacrificial layer reduces

https://doi.org/10.1021/acsaelm.3c00879
ACS Appl. Electron. Mater. XXXX, XXX, XXX−XXX

Table 1. Comparison of Communication Technologies for Implantable BCI Devices

Communication technologies	Propagation methods	Range	Frequency
Molecular communications	Propagation through axon, Action potential, Hormone distribution by blood, Ionic transportation	nm to μm	≤0.3 kHz[136]
Optical communications	Infrared propagation	<6.9 mm	300 GHz−430 THz[137]
Inductively coupled data transfer	Magnetic field or mutual inductance	≤4 cm	1 MHz[138] 5−49 MHz[139−141]
Intrabody communication (IBC)	Electric field	≤10 cm	Capacitive: 100 kHz − 150 MHz[142] Galvanic: <10 MHz[143]
Ultrasonic communication	Ultrasonic propagation	≤10 cm	1−3 MHz[144]
Antenna-based radio frequency	Radio wave propagation	2 m	415 MHz−1.18 GHz[145,146,147]

potential problems with twisting and wrinkling in free-standing microstructures, making it easier to print on flat polymer surfaces (such as polydimethylsiloxane).[130] Truong et al. developed a stamping-free micromachining process for 3D flexible and stretchable wide bandgap electronics. By using photolithography on both sides of free-standing nanomembranes, the method creates flexible structures on commercial silicon wafers, allowing for the customization of the material's optical transparency and mechanical properties.[131] Bose et al. developed a retrievable implant for therapeutic xenogeneic cells, which can work for over 130 days (Figure 5G).[132] Garcia-Cortadella et al. implanted a graphene active sensor array for mapping of a wide frequency band and epicortical brain signal. The system worked stably for up to 12 weeks (Figure 5H).[133] Devices made of this material have the following advantages. First, they can last for long-term measurement. A single surgery in many years allows for managing pain and cost associated with the surgery. Second, these materials are reliable to ensure long-term operation in the body. However, this material also has limitations of a challenging manufacturing process that requires high-end equipment. Zhang et al. developed a flexible and microendovascular (MEV) neural probe that can be implanted into sub-100-μm-scale blood vessels in the brains of rodents without open-skull surgery and damaging the brain or vasculature. The microcatheter, a flexible tube with an inner diameter of 200 μm and an outside diameter of 350 μm, can be rolled up inside the 900-μm-wide probe thanks to the transverse ribbons in the device region. In order to enable neuronal recording across vessel walls at single-cell resolution, the MEV probes can be inserted explicitly into small vessel branches that are inaccessible to any available microcatheters. The probe−tissue interface's histology investigations revealed a negligible immune response and long-term stability. Local field potentials and single-unit spikes have been selectively recorded using in vivo electrophysiology in the brain and olfactory bulb.[134] Luan et al. has developed nanoelectronic thread (NET) flexible electrodes with subcellular dimensions, and cellular surgical footprints form reliable, glial scar-free neural integration. The team fabricated two types of NET brain probes, NET-50 probes with electrodes 10-μm long and 10-μm wide and NET-10 20-μm long and 10-μm wide along the length of the probe. The team fabricated the multilayer probes using photolithography on a nickel metal release layer on a silicon substrate (n-type, 0.005 V·cm). The flexible neural probe was positioned on the surface of the brain where the dura mater had been removed. Using a 32-channel assessment system (Intan Technologies) with a bare Ag wire put into the contralateral hemisphere of the brain as the grounding reference, voltage signals from the neural electrodes were amplified and digitalized. The same tools measured the electrode's impedance at 1 kHz.[135]

5. COMMUNICATIONS AND POWERING FOR IMPLANTABLE BCI DEVICES

Power and communication technologies for BCI implantable devices are determined by the size, operation life, required cost, and fabrication technology. Furthermore, these technologies must meet the standards of safety and compatibility with external receivers such as suitable wavelength and transmission protocols.

5.1. Communication Schemes. Today's implantable BCI devices use various communication methods, also known as data transmission methods. Currently, the most popular communication methods are molecular communications, optical communications, inductively coupled data transfer, intrabody communication (IBC), ultrasonic communication, and antenna-based radio frequency. Table 1 provides an overview of popular communication technologies for implantable BCI devices, with their propagation methods, operation range, and frequency of electromagnetic waves. This is important information for researchers and companies to compare the differences and choose the appropriate communication technologies for their research and products.

First, molecular communication is a way of transmitting the information signal from the implantable device to the body through axon propagation, action potential, hormone distribution by blood, and ionic distribution through junction gap. Galluccio et al. provided a block model of the subsystems that make up a single neuron and defined their operation in terms of transfer functions to model neuronal system, with the goal of simulating the operation of biological neuron network. The team discovered that neurons normally filter neuronal stimuli in the range from 0 to 0.3 kHz by considering the cascade of the various blocks simulating the overall neuronal function. This mode has the smallest range, from only a few nm to μm, due to the nanoscale distance between cells.[136]

Second, implantable BCI devices can transmit data through optical communications. Information is transmitted with wavelengths in the infrared spectrum and an extensive transmission frequency from 300 GHz to 430THz. Abita et al. tested data transmission by optical communication through skin, in different parts such as eye, stomach, and back, with contact with thickness from 2.87 to 6.9 mm by LED with a wavelength of 880 nm.[137] The transmission distance of this type is relatively small, only up to 4 mm, because the light used has a long wavelength, so it cannot penetrate thick tissue layers.

https://doi.org/10.1021/acsaelm.3c00879
ACS Appl. Electron. Mater. XXXX, XXX, XXX−XXX

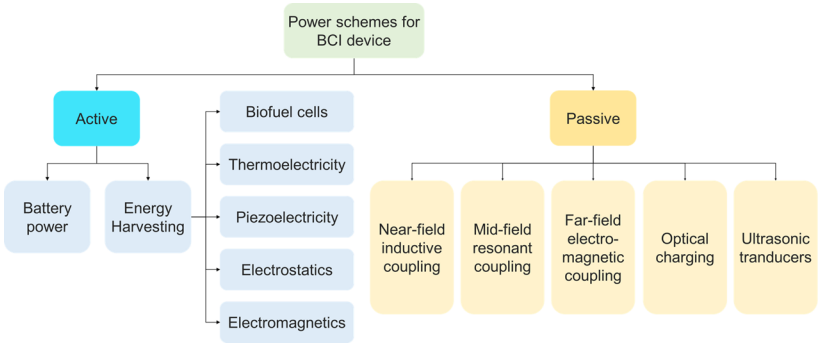

Figure 6. Powering schemes of implantable BCI devices.

Table 2. Comparison of Power Schemes for Implantable BCI Devices

Types of power technologies	Power technologies	Generated power	Advantages	Disadvantages
Battery powered system	Battery	Lithium-ion batteries: 1.85−74 mW[152]	Reasonable cost	Toxicity
		Lithium batteries: 210 Wh/kg[153]	Long service life (>10 years)	
Energy harvesting system	Biofuel cells	2.4 μW[154]	Recyclable materials	Short service life
			Biocompatibility with the human body	Low output power
				Low output voltage
	Thermoelectricity	106 μW/mK[2155,155,156]	Limitless service life	Low output power
	Piezoelectricity	0.33 μW[157]	High output power	Restricted human body locations to implant
			No required additional voltage source	
	Electrostatic	36 μW[158,159]	High output power	Additional voltage source
		58 μW[158,159]		High output impedance
		80 μW[160]		
	Electromagnetic	40−200 μW[161]	Limitless human body locations to implant	Complexity in fabrication technologies
		1.1 mW[162]		
Passively powered system	Near-field inductive coupling	6.15 mW[163]	High data rate and power transferring	Limited carrier frequency due to human tissue absorptions
		50 mW[164,165]	No batteries	
		150 mW[166]		
	Midfield resonant coupling	200 μW−500 mW[167]	Deep human implantable locations	Attenuation in tissue
	Far-field electromagnetic coupling	20.7−84.4 μW[168]	Deep human implantable locations	High attenuation in tissue
			High directivity	
	Optical charging	22 mW/cm[169]	High output power	Large size
			High efficiency	
	Ultrasonic transducer	1.5 mW/cm[2170]	Work efficiently with different depths	Low output power

Third, the most common method for data transfer in implantable BCI devices is inductively coupled data transfer. This mode of communication is based on magnetic field or mutual inductance, with frequencies ranging from 1 to 49 MHz and an average distance of up to 4 cm. This method can transmit data through tissue layers, from implantable devices to peripheral devices attached to the patient's skin, and then to a computer or an external database for further analysis. Wang et al. tested information transmission using an optimized coil pair driven by a Class-E power amplifier with a frequency of 1 MHz, from a microelectrode array to an external coil, that are 7 mm to 15 mm apart.[138] Ghovanloo et al. tested inductively powered wireless biomedical implants at a data rate in excess of 1 Mbps and frequency from 5 to 10 MHz.[139] Dawson et al. developed a 350 μW CMOS MSK transmitter and 400 μW OOK super-regenerative receiver. The transceiver is implemented in 90 nm CMOS and digitally tunes 24 MHz in frequency steps smaller than 2 kHz. The transmitter meets MICS mask specifications with data rates up to 120 kb/s consuming only 2.9 nJ/bit. The receiver has a sensitivity better than −99 dBm with a data rate of 40 kb/s or −93 dBm with a data rate of 120 kb/s consuming 3.3 nJ/bit.[140] Zeng et al. comapared the overall RF data transmission specifications in three major cochlear implant manufacturers. As such, Nucleus Freedom cochlear implants can transmit data with a carrier frequency of 5 MHz at a data rate of 500 KBits/s, and Med El Sonata implants have the transmission with a carrier frequency of 12 MHz at 600 KBits/s. Meanwhile, Clarion Hires 90K implants can transmit data with a frequency of 49 MHz at 1.09 MBits/s.[141]

https://doi.org/10.1021/acsaelm.3c00879
ACS Appl. Electron. Mater. XXXX, XXX, XXX−XXX

The fourth mode of communication is intrabody communication (IBC). This mode of communication is based on electric field in which implantable devices communicate with each other within a range of up to 10 cm. Cho et al. developed a distributed RC model with the frequency range from 100 kHz to 150 MHz with the body channel transceivers transmitting the signal in a current loop. The loop consists of the transmitter electrode, the body channel, and the receiver electrode and returns through the external ground. This system can transmit signals within a 1.2 m range.[142] Song et al. conducted simulation of the galvanic coupling intrabody communication with different signal transmission paths and a frequency range from 100 kHz to 5 MHz.[143]

Fifth, data can be communicated through ultrasound from the implantable BCI device to an external device. Mazzilli et al. developed an ultrasonic on−off keying/amplitude-shift keying demodulator using standard 0.18-μm CMOS technology. This demodulator involves a low-noise amplifier, variable gain amplifiers, an offset cancellation circuit, an envelope detector circuit, and a hysteresis comparator. The system transmits at a rate of 50 kb/s, a frequency of 1 MHz, a range of 10 cm, and a power consumption of 184 μW at a 1.5 V supply.[144]

The final communication method is a radio frequency-based antenna. This mode communicates at radio frequency. Zhang et al. reported antenna-based neural-recording systems using a frequency range between 415 MHz and 1.18 GHz, a data rate from 250 Kbits/s to 54.24 MBits/s, and a power consumption from 49.8 to 6600 μW.[145] Teshome et al. also reported that this communication method has the most extended range of up to 2 m.[146]

5.2. Powering Schemes. State-of-the-art implantable BCI devices use three main types of power supply technology: (i) battery, (ii) energy harvesting, and (iii) energy transfer. Figure 6 provides an overview of the powering schemes for implantable BCI devices currently in use and how manufacturers categorize them based on types of power supply technology.

One of the most common batteries in implantable BCI devices is lithium ion batteries with a lifespan of up to 10 years[148] and nuclear batteries that can last for more than 15 years. These systems have the advantage of long-term convenience, but require surgery for battery change.[149]

Energy harvesting utilizes biofuel, thermoelectricity, piezoelectricity, electric charge, and magnetism for various power ranges and durations as listed in Table 2. Depending on the operation time, durability, and size of the device, manufacturers can choose the appropriate power supply type. These systems offer great convenience to the patient as batteries change is eliminated. However, energy harvesting results in lower power and is more unreliable than the other two methods.[149]

Energy transfer uses technologies such as near-field inductive coupling, midfield resonant coupling, far-field electro-magnetic coupling, optical charging, and ultrasonic transducers[150,151] to transfer power to the device during its operation. This power concept expands the device operation and makes them more compact. However, this concept reduces patient's convenience because the patient has to be regularly in contact with an external energy transmitter.[149]

CONCLUSION AND PERSPECTIVES

Despite their recent emergence in the past two decades, flexible, implantable BCI devices have been making a significant leap from proof-of-concept to setting up baselines for clinical trials toward commercial products. Recently, soft conformal BCI electronics have been a game changer for solving the mechanical and geometrical mismatches between the implanted device and the tissue, minimizing the immunological response and side effects. Moreover, advances in smart materials and device integration would allow for a flexible device lifetime that meets the need of either temporary or long-term treatments. By engineering mechanical and electronic properties of the device materials, implantable BCI systems can dissolve after a given time frame, therefore eliminating the need for surgical removal. On the other hand, novel wide bandgap inorganic nanomaterials promise longevity and stability for devices that can serve the patient's entire life. Even though significant advancements have been achieved, considerable challenges persist and need to be addressed to bring soft implantable BCI devices to real-world applications and ready for commercialization: (i) Further innovations are needed in material and engineering to enhance material biocompatibility, to minimize foreign body responses, especially in long-term operation, and to make the device performance resistant from biofouling. (ii) Device encapsulation strategies are needed for long-term BCI to protect implanted electronics from corrosive biological environments. Reduced thickness and sandwich layers of BCI are preferred to enhance flexibility and conformability for tissue contacts. However, this also increases the permeability of ions into the sensitive electronics, reducing device performance and lifetime. Despite the limited choice for long-lived BCI platforms, wide bandgap nanobarriers can be a potential candidate for solving the dauting challenges of soft and long-lived components. Further research and development of this class of materials are still required. (iii) Energy efficient schemes are needed for power consumption and communication that allow for continuous and real-time operation of implanted BCIs.

In summary, we envision that soft implantable electronics will be the focus in the future of BCI technology due to their minimal invasiveness and tissue compatibility. This will be further strengthened by recent advances in materials and integration that push the current boundary in biomedical applications, enabling next-generation bioelectronics for precise therapeutics, disease diagnostics, and personalized healthcare.

AUTHOR INFORMATION

Corresponding Authors

Tuan-Khoa Nguyen − *Queensland Micro- and Nanotechnology Centre, Griffith University, Nathan, Queensland 4111, Australia;* orcid.org/0000-0003-1271-9576; Email: k.nguyentuan@griffith.edu.au

Nam-Trung Nguyen − *Queensland Micro- and Nanotechnology Centre, Griffith University, Nathan, Queensland 4111, Australia;* orcid.org/0000-0003-3626-5361; Email: nam-trung.nguyen@griffith.edu.au

Authors

Minh Anh Huynh − *Queensland Micro- and Nanotechnology Centre, Griffith University, Nathan, Queensland 4111, Australia*

Thanh-Ha Nguyen − *Queensland Micro- and Nanotechnology Centre, Griffith University, Nathan, Queensland 4111, Australia*

Complete contact information is available at:

https://doi.org/10.1021/acsaelm.3c00879
ACS Appl. Electron. Mater. XXXX, XXX, XXX−XXX

https://pubs.acs.org/10.1021/acsaelm.3c00879

Notes

The authors declare no competing financial interest.

■ ACKNOWLEDGMENTS

N.-T. Nguyen and M. A. Huynh acknowledge funding from the Australian Research Council (ARC) Discovery Project (Grant No. DP220100261) and ARC Laureate Fellowship (FL230100023). T.-K. Nguyen acknowledges funding through the Griffith University Postdoctoral Fellowship, New Researcher Grant, and ARC DECRA No. DE240100408. T.-H. Nguyen acknowledges the Australian Academy of Technological Sciences and Engineering for her Elevate Scholarship.

■ REFERENCES

(1) Yao, G.; Kang, L.; Li, J.; Long, Y.; Wei, H.; Ferreira, C. A.; Jeffery, J. J.; Lin, Y.; Cai, W.; Wang, X. Effective weight control via an implanted self-powered vagus nerve stimulation device. *Nat. Commun.* **2018**, *9* (1), 5349.

(2) Bonizzato, M.; Pidpruzhnykova, G.; DiGiovanna, J.; Shkorbatova, P.; Pavlova, N.; Micera, S.; Courtine, G. Brain-controlled modulation of spinal circuits improves recovery from spinal cord injury. *Nat. Commun.* **2018**, *9* (1), 3015.

(3) Ardell, J. L. Mechanisms of spinal cord neuromodulation for heart disease. *Nature Reviews Cardiology* **2016**, *13* (3), 127−128.

(4) Capogrosso, M.; Wagner, F. B.; Gandar, J.; Moraud, E. M.; Wenger, N.; Milekovic, T.; Shkorbatova, P.; Pavlova, N.; Musienko, P.; Bezard, E.; Bloch, J.; Courtine, G. Configuration of electrical spinal cord stimulation through real-time processing of gait kinematics. *Nat. Protoc.* **2018**, *13* (9), 2031−2061.

(5) Jackson, A. Neural interfaces take another step forward. *Nature* **2016**, *539* (7628), 177−178.

(6) Shanechi, M. M. Brain−machine interfaces from motor to mood. *Nature Neuroscience* **2019**, *22* (10), 1554−1564.

(7) Musk, E. An Integrated Brain-Machine Interface Platform With Thousands of Channels. *J. Med. Internet Res.* **2019**, *21* (10), No. e16194.

(8) Liu, Z.; Tang, J.; Gao, B.; Yao, P.; Li, X.; Liu, D.; Zhou, Y.; Qian, H.; Hong, B.; Wu, H. Neural signal analysis with memristor arrays towards high-efficiency brain−machine interfaces. *Nat. Commun.* **2020**, *11* (1), 4234.

(9) Ersaro, N. T.; Yalcin, C.; Muller, R. The future of brain−machine interfaces is optical. *Nature Electronics* **2023**, *6* (2), 96−98.

(10) Patel, M. A.; Zala, N. K.; Shah, P. A.; Murugan, N. S. Mind machine interface using internet of things. *Int. J. Res. EngSci. Manage* **2019**, *2*, 145.

(11) Sen, P.; Sarkar, H.; Bhattacharya, A. Technologies for Mind - Machine Interface. *Techno International Journal of Health, Engineering, Management & Science* **2018**, *2* (3), 84−94.

(12) Guan, J.; Hawryluk, G. W. J. Advancements in the mind-machine interface: towards re-establishment of direct cortical control of limb movement in spinal cord injury. *Neural Regeneration Research* **2016**, *11* (7), 1060−1061.

(13) Nielsen, C. B. Visualization: A Mind−Machine Interface for Discovery. *Trends in Genetics* **2016**, *32* (2), 73−75.

(14) Donoghue, J. P. Bridging the brain to the world: a perspective on neural interface systems. *Neuron* **2008**, *60* (3), 511−521.

(15) Won, S. M.; Song, E.; Zhao, J.; Li, J.; Rivnay, J.; Rogers, J. A. Recent Advances in Materials, Devices, and Systems for Neural Interfaces. *Adv. Mater.* **2018**, *30* (30), 1800534.

(16) Song, E.; Li, J.; Won, S. M.; Bai, W.; Rogers, J. A. Materials for flexible bioelectronic systems as chronic neural interfaces. *Nat. Mater.* **2020**, *19* (6), 590−603.

(17) Wellman, S. M.; Eles, J. R.; Ludwig, K. A.; Seymour, J. P.; Michelson, N. J.; McFadden, W. E.; Vazquez, A. L.; Kozai, T. D. Y. A Materials Roadmap to Functional Neural Interface Design. *Adv. Funct. Mater.* **2018**, *28* (12), 1701269.

(18) Acarón Ledesma, H.; Li, X.; Carvalho-de-Souza, J. L.; Wei, W.; Bezanilla, F.; Tian, B. An atlas of nano-enabled neural interfaces. *Nat. Nanotechnol.* **2019**, *14* (7), 645−657.

(19) Driscoll, N.; Richardson, A. G.; Maleski, K.; Anasori, B.; Adewole, O.; Lelyukh, P.; Escobedo, L.; Cullen, D. K.; Lucas, T. H.; Gogotsi, Y.; Vitale, F. Two-Dimensional Ti3C2MXene for High-Resolution Neural Interfaces. *ACS Nano* **2018**, *12* (10), 10419−10429.

(20) Clément, C. *Brain-Computer Interface Technologies*; Springer, 2019, 1−4. DOI: 10.1007/978-3-030-27852-6.

(21) Yu, K. J.; Kuzum, D.; Hwang, S.-W.; Kim, B. H.; Juul, H.; Kim, N. H.; Won, S. M.; Chiang, K.; Trumpis, M.; Richardson, A. G.; Cheng, H.; Fang, H.; Thompson, M.; Bink, H.; Talos, D.; Seo, K. J.; Lee, H. N.; Kang, S.-K.; Kim, J.-H.; Lee, J. Y.; Huang, Y.; Jensen, F. E.; Dichter, M. A.; Lucas, T. H.; Viventi, J.; Litt, B.; Rogers, J. A. Bioresorbable silicon electronics for transient spatiotemporal mapping of electrical activity from the cerebral cortex. *Nat. Mater.* **2016**, *15* (7), 782−791.

(22) Yang, Y.; Boling, S.; Mason, A. J. A Hardware-Efficient Scalable Spike Sorting Neural Signal Processor Module for Implantable High-Channel-Count Brain Machine Interfaces. *IEEE Transactions on Biomedical Circuits and Systems* **2017**, *11* (4), 743−754.

(23) Navas, M.; Navarrete, E. G.; Pascual, J. M.; Carrasco, R.; Núñez, J. A.; Shakur, S. F.; Pastor, J.; Sola, R. G. Treatment of refractory epilepsy in adult patients with right-sided vagus nerve stimulation. *Epilepsy Research* **2010**, *90* (1), 1−7.

(24) Toffa, D. H.; Touma, L.; El Meskine, T.; Bouthillier, A.; Nguyen, D. K. Learnings from 30 years of reported efficacy and safety of vagus nerve stimulation (VNS) for epilepsy treatment: A critical review. *Seizure* **2020**, *83*, 104−123.

(25) Habibagahi, I.; Omidbeigi, M.; Hadaya, J.; Lyu, H.; Jang, J.; Ardell, J. L.; Bari, A. A.; Babakhani, A. Vagus nerve stimulation using a miniaturized wirelessly powered stimulator in pigs. *Sci. Rep.* **2022**, *12* (1), 1−12.

(26) Libbus, I.; Stubbs, S. R.; Mazar, S. T.; Mindrebo, S.; KenKnight, B. H.; DiCarlo, L. A. Effect of defibrillation on the performance of an implantable vagus nerve stimulation system. *Bioelectronic Medicine* **2021**, *7* (1), 3.

(27) El Tahry, R.; Raedt, R.; Mollet, L.; De Herdt, V.; Wyckuys, T.; Van Dycke, A.; Meurs, A.; Dewaele, F.; Van Roost, D.; Doguet, P.; Delbeke, J.; Wadman, W.; Vonck, K.; Boon, P. A novel implantable vagus nerve stimulation system (ADNS-300) for combined stimulation and recording of the vagus nerve: Pilot trial at Ghent University Hospital. *Epilepsy Research* **2010**, *92* (2), 231−239.

(28) Langlois, L.; Antor, M.; Atmani, K.; Le Long, E.; Merriaux, P.; Bridoux, V.; Dechelotte, P.; Leroi, A. M.; Meleine, M.; Gourcerol, G. Development of a remote-controlled implantable rat sacral nerve stimulation system. *Neuromodulation: Technology at the Neural Interface* **2019**, *22* (6), 690−696.

(29) Deshmukh, A.; Brown, L.; Barbe, M. F.; Braverman, A. S.; Tiwari, E.; Hobson, L.; Shunmugam, S.; Armitage, O.; Hewage, E.; Ruggieri, M. R.; Morizio, J. Fully implantable neural recording and stimulation interfaces: Peripheral nerve interface applications. *Journal of Neuroscience Methods* **2020**, *333*, 108562.

(30) Woodington, B. J.; Curto, V. F.; Yu, Y.-L.; Martínez-Domínguez, H.; Coles, L.; Malliaras, G. G.; Proctor, C. M.; Barone, D. G. Electronics with shape actuation for minimally invasive spinal cord stimulation. *Science Advances* **2021**, *7* (26), No. eabg7833.

(31) Lorach, H.; Galvez, A.; Spagnolo, V.; Martel, F.; Karakas, S.; Intering, N.; Vat, M.; Faivre, O.; Harte, C.; Komi, S.; Ravier, J.; Collin, T.; Coquoz, L.; Sakr, I.; Baaklini, E.; Hernandez-Charpak, S. D.; Dumont, G.; Buschman, R.; Buse, N.; Denison, T.; van Nes, I.; Asboth, L.; Watrin, A.; Struber, L.; Sauter-Starace, F.; Langar, L.; Auboiroux, V.; Carda, S.; Chabardes, S.; Aksenova, T.; Demesmaeker, R.; Charvet, G.; Bloch, J.; Courtine, G. Walking naturally after spinal cord injury using a brain−spine interface. *Nature* **2023**, *618* (7963), 126−133.

(32) Anderson, M. A.; Squair, J. W.; Gautier, M.; Hutson, T. H.; Kathe, C.; Barraud, Q.; Bloch, J.; Courtine, G. Natural and targeted circuit reorganization after spinal cord injury. *Nature Neuroscience* **2022**, *25* (12), 1584−1596.
(33) Kathe, C.; Skinnider, M. A.; Hutson, T. H.; Regazzi, N.; Gautier, M.; Demesmaeker, R.; Komi, S.; Ceto, S.; James, N. D.; Cho, N.; Baud, L.; Galan, K.; Matson, K. J. E.; Rowald, A.; Kim, K.; Wang, R.; Minassian, K.; Prior, J. O.; Asboth, L.; Barraud, Q.; Lacour, S. P.; Levine, A. J.; Wagner, F.; Bloch, J.; Squair, J. W.; Courtine, G. The neurons that restore walking after paralysis. *Nature* **2022**, *611* (7936), 540−547.
(34) Greiner, N.; Barra, B.; Schiavone, G.; Lorach, H.; James, N.; Conti, S.; Kaeser, M.; Fallegger, F.; Borgognon, S.; Lacour, S.; Bloch, J.; Courtine, G.; Capogrosso, M. Recruitment of upper-limb motoneurons with epidural electrical stimulation of the cervical spinal cord. *Nat. Commun.* **2021**, *12* (1), 435.
(35) Jackson, A.; Zimmermann, J. B. Neural interfaces for the brain and spinal cord—restoring motor function. *Nature Reviews Neurology* **2012**, *8* (12), 690−699.
(36) Krauss, J. K.; Lipsman, N.; Aziz, T.; Boutet, A.; Brown, P.; Chang, J. W.; Davidson, B.; Grill, W. M.; Hariz, M. I.; Horn, A.; Schulder, M.; Mammis, A.; Tass, P. A.; Volkmann, J.; Lozano, A. M. Technology of deep brain stimulation: current status and future directions. *Nature Reviews Neurology* **2021**, *17* (2), 75−87.
(37) Cagnan, H.; Denison, T.; McIntyre, C.; Brown, P. Emerging technologies for improved deep brain stimulation. *Nat. Biotechnol.* **2019**, *37* (9), 1024−1033.
(38) Lin, Y. P.; Yeh, C. Y.; Huang, P. Y.; Wang, Z. Y.; Cheng, H. H.; Li, Y. T.; Chuang, C. F.; Huang, P. C.; Tang, K. T.; Ma, H. P.; Chang, Y. C.; Yeh, S. R.; Chen, H. A Battery-Less, Implantable Neuro-Electronic Interface for Studying the Mechanisms of Deep Brain Stimulation in Rat Models. *IEEE Transactions on Biomedical Circuits and Systems* **2016**, *10* (1), 98−112.
(39) Hwang, G.-T.; Kim, Y.; Lee, J.-H.; Oh, S.; Jeong, C. K.; Park, D. Y.; Ryu, J.; Kwon, H.; Lee, S.-G.; Joung, B.; Kim, D.; Lee, K. J. Self-powered deep brain stimulation via a flexible PIMNT energy harvester. *Energy Environ. Sci.* **2015**, *8* (9), 2677−2684.
(40) Bodart, C.; Rossetti, N.; Hagler, J. E.; Chevreau, P.; Chhin, D.; Soavi, F.; Schougaard, S. B.; Amzica, F.; Cicoira, F. Electropolymerized Poly(3,4-ethylenedioxythiophene) (PEDOT) Coatings for Implantable Deep-Brain-Stimulating Microelectrodes. *ACS Appl. Mater. Interfaces* **2019**, *11* (19), 17226−17233.
(41) Lozano, A. M.; Lipsman, N.; Bergman, H.; Brown, P.; Chabardes, S.; Chang, J. W.; Matthews, K.; McIntyre, C. C.; Schlaepfer, T. E.; Schulder, M.; Temel, Y.; Volkmann, J.; Krauss, J. K. Deep brain stimulation: current challenges and future directions. *Nature Reviews Neurology* **2019**, *15* (3), 148−160.
(42) Kozielski, K. L.; Jahanshahi, A.; Gilbert, H. B.; Yu, Y.; Erin, Ö.; Francisco, D.; Alosaimi, F.; Temel, Y.; Sitti, M. Nonresonant powering of injectable nanoelectrodes enables wireless deep brain stimulation in freely moving mice. *Science Advances* **2021**, *7* (3), No. eabc4189.
(43) Corridon, P. R.; Ko, I. K.; Yoo, J. J.; Atala, A. Bioartificial Kidneys. *Current Stem Cell Reports* **2017**, *3* (2), 68−76.
(44) Won, S. M.; Song, E.; Reeder, J. T.; Rogers, J. A. Emerging Modalities and Implantable Technologies for Neuromodulation. *Cell* **2020**, *181* (1), 115−135.
(45) Jung, Y. H.; Kim, J. U.; Lee, J. S.; Shin, J. H.; Jung, W.; Ok, J.; Kim, T.-i. Injectable Biomedical Devices for Sensing and Stimulating Internal Body Organs. *Adv. Mater.* **2020**, *32* (16), 1907478.
(46) McGee, M. J.; Amundsen, C. L.; Grill, W. M. Electrical stimulation for the treatment of lower urinary tract dysfunction after spinal cord injury. *Journal of Spinal Cord Medicine* **2015**, *38* (2), 135−146.
(47) Zheng, Q.; Tang, Q.; Wang, Z. L.; Li, Z. Self-powered cardiovascular electronic devices and systems. *Nature Reviews Cardiology* **2021**, *18* (1), 7−21.
(48) Naples, J. G.; Ruckenstein, M. J. Cochlear implant. *Otolaryngologic Clinics of North America* **2020**, *53* (1), 87−102.
(49) Riggs, W. J.; Hiss, M. M.; Skidmore, J.; Varadarajan, V. V.; Mattingly, J. K.; Moberly, A. C.; Adunka, O. F. Utilizing Electrocochleography as a Microphone for Fully Implantable Cochlear Implants. *Sci. Rep.* **2020**, *10* (1), 3714.
(50) İlik, B.; Koyuncuoğlu, A.; Şardan-Sukas, Ö.; Külah, H. Thin film piezoelectric acoustic transducer for fully implantable cochlear implants. *Sensors and Actuators A: Physical* **2018**, *280*, 38−46.
(51) Külah, H.; Uluşan, H.; Chamanian, S.; Batu, A.; Uğur, M. B.; Yüksel, M. B.; Yilmaz, A. M.; Yiğit, H. A.; Koyuncuoğlu, A.; Ö, T.; Soydan, A. K. A Fully-Implantable Mems-Based Autonomous Cochlear Implant. In *2022 IEEE 35th International Conference on Micro Electro Mechanical Systems Conference (MEMS)*, 2022; pp 396−399. DOI: 10.1109/MEMS51670.2022.9699689.
(52) Xu, H.; Zhong, X.; Pang, C.; Zou, J.; Chen, W.; Wang, X.; Li, S.; Hu, Y.; Sagan, D. S.; Weiss, P. T.; Yao, Y.; Xiang, J.; Dayan, M. S.; Humayun, M. S.; Tai, Y.-C. First human results with the 256 channel Intelligent Micro Implant Eye (IMIE 256). *Translational Vision Science & Technology* **2021**, *10* (10), 14−14.
(53) Zeng, Q.; Zhao, S.; Yang, H.; Zhang, Y.; Wu, T. Micro/Nano Technologies for High-Density Retinal Implant. *Micromachines* **2019**, *10*, 419.
(54) Mills, J. O.; Jalil, A.; Stanga, P. E. Electronic retinal implants and artificial vision: journey and present. *Eye* **2017**, *31* (10), 1383−1398.
(55) Jiang, L.; Lu, G.; Zeng, Y.; Sun, Y.; Kang, H.; Burford, J.; Gong, C.; Humayun, M. S.; Chen, Y.; Zhou, Q. Flexible ultrasound-induced retinal stimulating piezo-arrays for biomimetic visual prostheses. *Nat. Commun.* **2022**, *13* (1), 3853.
(56) Benfenati, F.; Lanzani, G. New technologies for developing second generation retinal prostheses. *Lab Animal* **2018**, *47* (3), 71−75.
(57) Lorach, H.; Goetz, G.; Smith, R.; Lei, X.; Mandel, Y.; Kamins, T.; Mathieson, K.; Huie, P.; Harris, J.; Sher, A.; Palanker, D. Photovoltaic restoration of sight with high visual acuity. *Nature Medicine* **2015**, *21* (5), 476−482.
(58) Cuttaz, E. A.; Chapman, C. A. R.; Syed, O.; Goding, J. A.; Green, R. A. Stretchable, fully polymeric electrode arrays for peripheral nerve stimulation. *Advanced Science* **2021**, *8* (8), 2004033.
(59) Eggenberger, S. C.; James, N. L.; Ho, C.; Eamegdool, S. S.; Tatarinoff, V.; Craig, N. A.; Gow, B. S.; Wan, S.; Dodds, C. W. D.; La Hood, D.; Gilmour, A.; Donahoe, S. L.; Krockenberger, M.; Tumuluri, K.; da Cruz, M. J.; Grigg, J. R.; McCluskey, P.; Lovell, N. H.; Madigan, M. C.; Fung, A. T.; Suaning, G. J. Implantation and long-term assessment of the stability and biocompatibility of a novel 98 channel suprachoroidal visual prosthesis in sheep. *Biomaterials* **2021**, *279*, 121191.
(60) Liu, J.; Fu, T.-M.; Cheng, Z.; Hong, G.; Zhou, T.; Jin, L.; Duvvuri, M.; Jiang, Z.; Kruskal, P.; Xie, C.; Suo, Z.; Fang, Y.; Lieber, C. M. Syringe-injectable electronics. *Nat. Nanotechnol.* **2015**, *10* (7), 629−636.
(61) Deep, N. L.; Dowling, E. M.; Jethanamest, D.; Carlson, M. L. Cochlear implantation: an overview. *Journal of Neurological Surgery Part B: Skull Base* **2019**, *80* (02), 169−177.
(62) Song, Y.; Min, J.; Gao, W. Wearable and Implantable Electronics: Moving toward Precision Therapy. *ACS Nano* **2019**, *13* (11), 12280−12286.
(63) Zhao, Z.; Spyropoulos, G. D.; Cea, C.; Gelinas, J. N.; Khodagholy, D. Ionic communication for implantable bioelectronics. *Science Advances* **2022**, *8* (14), No. eabm7851.
(64) Liu, Y.; Feig, V. R.; Bao, Z. Conjugated Polymer for Implantable Electronics toward Clinical Application. *Adv. Healthcare Mater.* **2021**, *10* (17), 2001916.
(65) El Shatanofy, M.; Hofmann, K.; Myseros, J. S.; Gaillard, W. D.; Keating, R. F.; Oluigbo, C. Invasive Intracranial Electroencephalogram (EEG) Monitoring for Epilepsy in the Pediatric Patient With a Shunt. *Cureus* **2023**, *15* (2), e35279.
(66) Sauter-Starace, F.; Ratel, D.; Cretallaz, C.; Foerster, M.; Lambert, A.; Gaude, C.; Costecalde, T.; Bonnet, S.; Charvet, G.; Aksenova, T.; Mestais, C.; Benabid, A.-L.; Torres-Martinez, N. Long-

https://doi.org/10.1021/acsaelm.3c00879
ACS Appl. Electron. Mater. XXXX, XXX, XXX−XXX

term sheep implantation of wimagine®, a wireless 64-channel electrocorticogram recorder. *Frontiers in Neuroscience* **2019**, *13*, 847.
(67) Shi, C.; Andino-Pavlovsky, V.; Lee, S. A.; Costa, T.; Elloian, J.; Konofagou, E. E.; Shepard, K. L. Application of a sub−0.1-mm3 implantable mote for in vivo real-time wireless temperature sensing. *Science Advances* **2021**, *7* (19), No. eabf6312.
(68) Song, E.; Li, R.; Jin, X.; Du, H.; Huang, Y.; Zhang, J.; Xia, Y.; Fang, H.; Lee, Y. K.; Yu, K. J.; Chang, J.-K.; Mei, Y.; Alam, M. A.; Huang, Y.; Rogers, J. A. Ultrathin Trilayer Assemblies as Long-Lived Barriers against Water and Ion Penetration in Flexible Bioelectronic Systems. *ACS Nano* **2018**, *12* (10), 10317−10326.
(69) Yoo, S.; Lee, J.; Joo, H.; Sunwoo, S.-H.; Kim, S.; Kim, D.-H. Wireless Power Transfer and Telemetry for Implantable Bioelectronics. *Adv. Healthcare Mater.* **2021**, *10* (17), 2100614.
(70) Li, Y.; Li, N.; De Oliveira, N.; Wang, S. Implantable bioelectronics toward long-term stability and sustainability. *Matter* **2021**, *4* (4), 1125−1141.
(71) Jang, T.-M.; Lee, J. H.; Zhou, H.; Joo, J.; Lim, B. H.; Cheng, H.; Kim, S. H.; Kang, I.-S.; Lee, K.-S.; Park, E.; Hwang, S.-W. Expandable and implantable bioelectronic complex for analyzing and regulating real-time activity of the urinary bladder. *Science Advances* **2020**, *6* (46), No. eabc9675.
(72) Lu, D.; Li, S.; Yang, Q.; Arafa, H. M.; Xu, Y.; Yan, Y.; Ostojich, D.; Bai, W.; Guo, H.; Wu, C.; Li, S.; Jacobson, L.; Westman, A. M.; MacEwan, M. R.; Huang, Y.; Pet, M.; Rogers, J. A. Implantable, wireless, self-fixing thermal sensors for continuous measurements of microvascular blood flow in flaps and organ grafts. *Biosens. Bioelectron.* **2022**, *206*, 114145.
(73) Kim, D.-H.; Ghaffari, R.; Lu, N.; Wang, S.; Lee, S. P.; Keum, H.; D'Angelo, R.; Klinker, L.; Su, Y.; Lu, C.; Kim, Y.-S.; Ameen, A.; Li, Y.; Zhang, Y.; de Graff, B.; Hsu, Y.-Y.; Liu, Z.; Ruskin, J.; Xu, L.; Lu, C.; Omenetto, F. G.; Huang, Y.; Mansour, M.; Slepian, M. J.; Rogers, J. A. Electronic sensor and actuator webs for large-area complex geometry cardiac mapping and therapy. *Proc. Natl. Acad. Sci. U. S. A.* **2012**, *109* (49), 19910−19915.
(74) Chen, R.; Canales, A.; Anikeeva, P. Neural recording and modulation technologies. *Nature Reviews Materials* **2017**, *2* (2), 16093.
(75) Silverå Ejneby, M.; Jakešová, M.; Ferrero, J. J.; Migliaccio, L.; Sahalianov, I.; Zhao, Z.; Berggren, M.; Khodagholy, D.; Đerek, V.; Gelinas, J. N.; Głowacki, E. D. Chronic electrical stimulation of peripheral nerves via deep-red light transduced by an implanted organic photocapacitor. *Nature Biomedical Engineering* **2022**, *6* (6), 741−753.
(76) Someya, T.; Bao, Z.; Malliaras, G. G. The rise of plastic bioelectronics. *Nature* **2016**, *540* (7633), 379−385.
(77) Ashok, A.; Nguyen, T.-K.; Barton, M.; Leitch, M.; Masud, M. K.; Park, H.; Truong, T.-A.; Kaneti, Y. V.; Ta, H. T.; Li, X.; Liang, K.; Do, T. N.; Wang, C.-H.; Nguyen, N.-T.; Yamauchi, Y.; Phan, H.-P. Flexible Nanoarchitectonics for Biosensing and Physiological Monitoring Applications. *Small* **2023**, *19* (9), 2204946.
(78) Nguyen, T.-K.; Yadav, S.; Truong, T.-A.; Han, M.; Barton, M.; Leitch, M.; Guzman, P.; Dinh, T.; Ashok, A.; Vu, H.; Dau, V.; Haasmann, D.; Chen, L.; Park, Y.; Do, T. N.; Yamauchi, Y.; Rogers, J. A.; Nguyen, N.-T.; Phan, H.-P. Integrated, Transparent Silicon Carbide Electronics and Sensors for Radio Frequency Biomedical Therapy. *ACS Nano* **2022**, *16* (7), 10890−10903.
(79) *BioRender*, 2023. https://www.biorender.com/.
(80) *flaticon*, 2023. https://www.flaticon.com/.
(81) Jun, J. J.; Steinmetz, N. A.; Siegle, J. H.; Denman, D. J.; Bauza, M.; Barbarits, B.; Lee, A. K.; Anastassiou, C. A.; Andrei, A.; Aydın, Ç.; Barbic, M.; Blanche, T. J.; Bonin, V.; Couto, J.; Dutta, B.; Gratiy, S. L.; Gutnisky, D. A.; Häusser, M.; Karsh, B.; Ledochowitsch, P.; Lopez, C. M.; Mitelut, C.; Musa, S.; Okun, M.; Pachitariu, M.; Putzeys, J.; Rich, P. D.; Rossant, C.; Sun, W.-l.; Svoboda, K.; Carandini, M.; Harris, K. D.; Koch, C.; O'Keefe, J.; Harris, T. D. Fully integrated silicon probes for high-density recording of neural activity. *Nature* **2017**, *551* (7679), 232−236.
(82) Angotzi, G. N.; Boi, F.; Lecomte, A.; Miele, E.; Malerba, M.; Zucca, S.; Casile, A.; Berdondini, L. SiNAPS: An implantable active pixel sensor CMOS-probe for simultaneous large-scale neural recordings. *Biosens. Bioelectron.* **2019**, *126*, 355−364.
(83) Deku, F.; Cohen, Y.; Joshi-Imre, A.; Kanneganti, A.; Gardner, T. J.; Cogan, S. F. Amorphous silicon carbide ultramicroelectrode arrays for neural stimulation and recording. *Journal of neural engineering* **2018**, *15* (1), 016007.
(84) Fu, T.-M.; Hong, G.; Zhou, T.; Schuhmann, T. G.; Viveros, R. D.; Lieber, C. M. Stable long-term chronic brain mapping at the single-neuron level. *Nat. Methods* **2016**, *13* (10), 875−882.
(85) Hong, G.; Yang, X.; Zhou, T.; Lieber, C. M. Mesh electronics: a new paradigm for tissue-like brain probes. *Current Opinion in Neurobiology* **2018**, *50*, 33−41.
(86) Fu, T.-M.; Hong, G.; Viveros, R. D.; Zhou, T.; Lieber, C. M. Highly scalable multichannel mesh electronics for stable chronic brain electrophysiology. *Proc. Natl. Acad. Sci. U. S. A.* **2017**, *114* (47), E10046−E10055.
(87) Liu, Y.; Liu, Z.; Zhou, Y.; Tian, Y. Implantable Electrochemical Sensors for Brain Research. *JACS Au* **2023**, *3* (6), 1572−1582.
(88) Wei, X.; Luan, L.; Zhao, Z.; Li, X.; Zhu, H.; Potnis, O.; Xie, C. Nanofabricated Ultraflexible Electrode Arrays for High-Density Intracortical Recording. *Advanced Science* **2018**, *5* (6), 1700625.
(89) Sohal, H.; Jackson, A.; Jackson, R.; Clowry, G.; Vassilevski, K.; O'Neill, A.; Baker, S. The Sinusoidal Probe: a new approach to improve electrode longevity. *Frontiers in neuroengineering* **2014**, *7*, 10.
(90) Boehler, C.; Kleber, C.; Martini, N.; Xie, Y.; Dryg, I.; Stieglitz, T.; Hofmann, U. G.; Asplund, M. Actively controlled release of Dexamethasone from neural microelectrodes in a chronic in vivo study. *Biomaterials* **2017**, *129*, 176−187.
(91) Guan, S.; Wang, J.; Gu, X.; Zhao, Y.; Hou, R.; Fan, H.; Zou, L.; Gao, L.; Du, M.; Li, C.; Fang, Y. Elastocapillary self-assembled neurotassels for stable neural activity recordings. *Science Advances* **2019**, *5* (3), No. eaav2842.
(92) Chen, C.-H.; Chuang, S.-C.; Lee, Y.-T.; Chang, Y.-C.; Yeh, S.-R.; Yao, D.-J. Three-dimensional flexible microprobe for recording the neural signal. *Journal of Micro/Nanolithography, MEMS and MOEMS* **2010**, *9* (3), 031007.
(93) Lecomte, A.; Castagnola, V.; Descamps, E.; Dahan, L.; Blatché, M.-C.; Dinis, T. M.; Leclerc, E.; Egles, C.; Bergaud, C. Silk and PEG as means to stiffen a parylene probe for insertion in the brain: toward a double time-scale tool for local drug delivery. *Journal of Micromechanics and Microengineering* **2015**, *25* (12), 125003.
(94) Wang, Y.; Yang, X.; Zhang, X.; Wang, Y.; Pei, W. Implantable intracortical microelectrodes: reviewing the present with a focus on the future. *Microsystems & Nanoengineering* **2023**, *9* (1), 7.
(95) Zhou, T.; Hong, G.; Fu, T.-M.; Yang, X.; Schuhmann, T. G.; Viveros, R. D.; Lieber, C. M. Syringe-injectable mesh electronics integrate seamlessly with minimal chronic immune response in the brain. *Proc. Natl. Acad. Sci. U. S. A.* **2017**, *114* (23), 5894−5899.
(96) Hong, Y. J.; Jeong, H.; Cho, K. W.; Lu, N.; Kim, D. H. Wearable and implantable devices for cardiovascular healthcare: from monitoring to therapy based on flexible and stretchable electronics. *Adv. Funct. Mater.* **2019**, *29* (19), 1808247.
(97) Nguyen, T.-K.; Barton, M.; Ashok, A.; Truong, T.-A.; Yadav, S.; Leitch, M.; Nguyen, T.-V.; Kashaninejad, N.; Dinh, T.; Hold, L.; Yamauchi, Y.; Nguyen, N.-T.; Phan, H.-P. Wide bandgap semiconductor nanomembranes as a long-term biointerface for flexible, implanted neuromodulator. *Proc. Natl. Acad. Sci. U. S. A.* **2022**, *119* (33), No. e2203287119.
(98) Kim, D.-H.; Viventi, J.; Amsden, J. J.; Xiao, J.; Vigeland, L.; Kim, Y.-S.; Blanco, J. A.; Panilaitis, B.; Frechette, E. S.; Contreras, D.; Kaplan, D. L.; Omenetto, F. G.; Huang, Y.; Hwang, K.-C.; Zakin, M. R.; Litt, B.; Rogers, J. A. Dissolvable films of silk fibroin for ultrathin conformal bio-integrated electronics. *Nat. Mater.* **2010**, *9* (6), 511−517.
(99) Xu, L.; Gutbrod, S. R.; Bonifas, A. P.; Su, Y.; Sulkin, M. S.; Lu, N.; Chung, H.-J.; Jang, K.-I.; Liu, Z.; Ying, M.; Lu, C.; Webb, R. C.; Kim, J.-S.; Laughner, J. I.; Cheng, H.; Liu, Y.; Ameen, A.; Jeong, J.-W.;

https://doi.org/10.1021/acsaelm.3c00879
ACS Appl. Electron. Mater. XXXX, XXX, XXX−XXX

Kim, G.-T.; Huang, Y.; Efimov, I. R.; Rogers, J. A. 3D multifunctional integumentary membranes for spatiotemporal cardiac measurements and stimulation across the entire epicardium. *Nat. Commun.* **2014**, *5* (1), 3329.
(100) Lu, W.; Bai, W.; Zhang, H.; Xu, C.; Chiarelli, A. M.; Vázquez-Guardado, A.; Xie, Z.; Shen, H.; Nandoliya, K.; Zhao, H.; Lee, K.; Wu, Y.; Franklin, D.; Avila, R.; Xu, S.; Rwei, A.; Han, M.; Kwon, K.; Deng, Y.; Yu, X.; Thorp, E. B.; Feng, X.; Huang, Y.; Forbess, J.; Ge, Z.-D.; Rogers, J. A. Wireless, implantable catheter-type oximeter designed for cardiac oxygen saturation. *Science Advances* **2021**, *7* (7), No. eabe0579.
(101) Park, S.; Guo, Y.; Jia, X.; Choe, H. K.; Grena, B.; Kang, J.; Park, J.; Lu, C.; Canales, A.; Chen, R.; Yim, Y. S.; Choi, G. B.; Fink, Y.; Anikeeva, P. One-step optogenetics with multifunctional flexible polymer fibers. *Nature Neuroscience* **2017**, *20* (4), 612−619.
(102) Wan, X.; Chen, P.; Xu, Z.; Mo, X.; Jin, H.; Yang, W.; Wang, S.; Duan, J.; Hu, B.; Luo, Z.; Huang, L.; Zhou, J. Hybrid-Piezoelectret Based Highly Efficient Ultrasonic Energy Harvester for Implantable Electronics. *Adv. Funct. Mater.* **2022**, *32* (24), 2200589.
(103) Capogrosso, M.; Milekovic, T.; Borton, D.; Wagner, F.; Moraud, E. M.; Mignardot, J.-B.; Buse, N.; Gandar, J.; Barraud, Q.; Xing, D.; Rey, E.; Duis, S.; Jianzhong, Y.; Ko, W. K. D.; Li, Q.; Detemple, P.; Denison, T.; Micera, S.; Bezard, E.; Bloch, J.; Courtine, G. A brain−spine interface alleviating gait deficits after spinal cord injury in primates. *Nature* **2016**, *539* (7628), 284−288.
(104) Yang, Q.; Wei, T.; Yin, R. T.; Wu, M.; Xu, Y.; Koo, J.; Choi, Y. S.; Xie, Z.; Chen, S. W.; Kandela, I.; Yao, S.; Deng, Y.; Avila, R.; Liu, T.-L.; Bai, W.; Yang, Y.; Han, M.; Zhang, Q.; Haney, C. R.; Benjamin Lee, K.; Aras, K.; Wang, T.; Seo, M.-H.; Luan, H.; Lee, S. M.; Brikha, A.; Ghoreishi-Haack, N.; Tran, L.; Stepien, I.; Aird, F.; Waters, E. A.; Yu, X.; Banks, A.; Trachiotis, G. D.; Torkelson, J. M.; Huang, Y.; Kozorovitskiy, Y.; Efimov, I. R.; Rogers, J. A. Photocurable bioresorbable adhesives as functional interfaces between flexible bioelectronic devices and soft biological tissues. *Nat. Mater.* **2021**, *20* (11), 1559−1570.
(105) Sun, Y.; Chao, S.; Ouyang, H.; Zhang, W.; Luo, W.; Nie, Q.; Wang, J.; Luo, C.; Ni, G.; Zhang, L.; Yang, J.; Feng, H.; Mao, G.; Li, Z. Hybrid nanogenerator based closed-loop self-powered low-level vagus nerve stimulation system for atrial fibrillation treatment. *Science Bulletin* **2022**, *67* (12), 1284−1294.
(106) Wright, J. P.; Mughrabi, I. T.; Wong, J.; Mathew, J.; Jayaprakash, N.; Crosfield, C.; Chang, E. H.; Chavan, S. S.; Tracey, K. J.; Pavlov, V. A.; Al-Abed, Y.; Zanos, T. P.; Zanos, S.; Datta-Chaudhuri, T. A fully implantable wireless bidirectional neuromodulation system for mice. *Biosens. Bioelectron.* **2022**, *200*, 113886.
(107) Cogan, S. F. Neural Stimulation and Recording Electrodes. *Annu. Rev. Biomed. Eng.* **2008**, *10* (1), 275−309.
(108) Kozai, T. D. Y.; Langhals, N. B.; Patel, P. R.; Deng, X.; Zhang, H.; Smith, K. L.; Lahann, J.; Kotov, N. A.; Kipke, D. R. Ultrasmall implantable composite microelectrodes with bioactive surfaces for chronic neural interfaces. *Nat. Mater.* **2012**, *11* (12), 1065−1073.
(109) Wang, K.; Frewin, C. L.; Esrafilzadeh, D.; Yu, C.; Wang, C.; Pancrazio, J. J.; Romero-Ortega, M.; Jalili, R.; Wallace, G. High-Performance Graphene-Fiber-Based Neural Recording Microelectrodes. *Adv. Mater.* **2019**, *31* (15), 1805867.
(110) Sohn, W. J.; Lim, J.; Wang, P. T.; Pu, H.; Malekzadeh-Arasteh, O.; Shaw, S. J.; Armacost, M.; Gong, H.; Kellis, S.; Andersen, R. A.; Liu, C. Y.; Heydari, P.; Nenadic, Z.; Do, A. H. Benchtop and bedside validation of a low-cost programmable cortical stimulator in a testbed for bi-directional brain-computer-interface research. *Frontiers in Neuroscience* **2023**, *16*, 1075971.
(111) Ye, T.; Lai, Y.; Wang, Z.; Zhang, X.; Meng, G.; Zhou, L.; Zhang, Y.; Zhou, Z.; Deng, J.; Wang, M.; Wang, Y.; Zhang, Q.; Zhou, X.; Yu, L.; Jiang, H.; Xiao, X. Precise Modulation of Gold Nanorods for Protecting against Malignant Ventricular Arrhythmias via Near-Infrared Neuromodulation. *Adv. Funct. Mater.* **2019**, *29* (36), 1902128.
(112) Wu, F.; Stark, E.; Ku, P.-C.; Wise, K. D.; Buzsaki, G.; Yoon, E. Monolithically Integrated μLEDs on Silicon Neural Probes for High-Resolution Optogenetic Studies in Behaving Animals. *Neuron* **2015**, *88* (6), 1136−1148.
(113) Chung, H.-J.; Sulkin, M. S.; Kim, J.-S.; Goudeseune, C.; Chao, H.-Y.; Song, J. W.; Yang, S. Y.; Hsu, Y.-Y.; Ghaffari, R.; Efimov, I. R.; Rogers, J. A. Stretchable, multiplexed pH sensors with demonstrations on rabbit and human hearts undergoing ischemia. *Adv. Healthcare Mater.* **2014**, *3* (1), 59−68.
(114) Kim, S. J.; Cho, K. W.; Cho, H. R.; Wang, L.; Park, S. Y.; Lee, S. E.; Hyeon, T.; Lu, N.; Choi, S. H.; Kim, D. H. Stretchable and transparent biointerface using cell-sheet−graphene hybrid for electrophysiology and therapy of skeletal muscle. *Adv. Funct. Mater.* **2016**, *26* (19), 3207−3217.
(115) Kim, D.-H.; Viventi, J.; Amsden, J. J.; Xiao, J.; Vigeland, L.; Kim, Y.-S.; Blanco, J. A.; Panilaitis, B.; Frechette, E. S.; Contreras, D.; Kaplan, D. L.; Omenetto, F. G.; Huang, Y.; Hwang, K.-C.; Zakin, M. R.; Litt, B.; Rogers, J. A. Dissolvable films of silk fibroin for ultrathin conformal bio-integrated electronics. *Nature materials* **2010**, *9* (6), 511−517.
(116) Takamatsu, T.; Sijie, Y.; Miyake, T. Wearable, Implantable, Parity-Time Symmetric Bioresonators for Extremely Small Biological Signal Monitoring. *Advanced Materials Technologies* **2023**, *8* (9), 2201704.
(117) Bai, W.; Shin, J.; Fu, R.; Kandela, I.; Lu, D.; Ni, X.; Park, Y.; Liu, Z.; Hang, T.; Wu, D.; Liu, Y.; Haney, C. R.; Stepien, I.; Yang, Q.; Zhao, J.; Nandoliya, K. R.; Zhang, H.; Sheng, X.; Yin, L.; MacRenaris, K.; Brikha, A.; Aird, F.; Pezhouh, M.; Hornick, J.; Zhou, W.; Rogers, J. A. Bioresorbable photonic devices for the spectroscopic characterization of physiological status and neural activity. *Nature Biomedical Engineering* **2019**, *3* (8), 644−654.
(118) Herbert, R.; Lim, H.-R.; Rigo, B.; Yeo, W.-H. Fully implantable wireless batteryless vascular electronics with printed soft sensors for multiplex sensing of hemodynamics. *Science Advances* **2022**, *8* (19), No. eabm1175.
(119) Dual, S. A.; Llerena Zambrano, B.; Sundermann, S.; Cesarovic, N.; Kron, M.; Magkoutas, K.; Hengsteler, J.; Falk, V.; Starck, C.; Meboldt, M.; Voros, J.; Schmid Daners, M. Continuous heart volume monitoring by fully implantable soft strain sensor. *Adv. Healthcare Mater.* **2020**, *9* (19), 2000855.
(120) Ferlauto, L.; Vagni, P.; Fanelli, A.; Zollinger, E. G.; Monsorno, K.; Paolicelli, R. C.; Ghezzi, D. All-polymeric transient neural probe for prolonged in-vivo electrophysiological recordings. *Biomaterials* **2021**, *274*, 120889.
(121) Guo, H.; Bai, W.; Ouyang, W.; Liu, Y.; Wu, C.; Xu, Y.; Weng, Y.; Zang, H.; Liu, Y.; Jacobson, L.; Hu, Z.; Wang, Y.; Arafa, H. M.; Yang, Q.; Lu, D.; Li, S.; Zhang, L.; Xiao, X.; Vázquez-Guardado, A.; Ciatti, J.; Dempsey, E.; Ghoreishi-Haack, N.; Waters, E. A.; Haney, C. R.; Westman, A. M.; MacEwan, M. R.; Pet, M. A.; Rogers, J. A. Wireless implantable optical probe for continuous monitoring of oxygen saturation in flaps and organ grafts. *Nat. Commun.* **2022**, *13* (1), 3009.
(122) Phan, H.-P. Implanted Flexible Electronics: Set Device Lifetime with Smart Nanomaterials. *Micromachines* **2021**, *12* (2), 157.
(123) Bai, W.; Shin, J.; Fu, R.; Kandela, I.; Lu, D.; Ni, X.; Park, Y.; Liu, Z.; Hang, T.; Wu, D.; Liu, Y.; Haney, C. R.; Stepien, I.; Yang, Q.; Zhao, J.; Nandoliya, K. R.; Zhang, H.; Sheng, X.; Yin, L.; MacRenaris, K.; Brikha, A.; Aird, F.; Pezhouh, M.; Hornick, J.; Zhou, W.; Rogers, J. A. Bioresorbable photonic devices for the spectroscopic characterization of physiological status and neural activity. *Nat. Biomed. Eng.* **2019**, *3* (8), 644−654.
(124) Lee, G.; Ray, E.; Yoon, H.-J.; Genovese, S.; Choi, Y. S.; Lee, M.-K.; Sahin, S.; Yan, Y.; Ahn, H.-Y.; Bandodkar, A. J.; Kim, J.; Park, M.; Ryu, H.; Kwak, S. S.; Jung, Y. H.; Odabas, A.; Khandpur, U.; Ray, W. Z.; MacEwan, M. R.; Rogers, J. A. A bioresorbable peripheral nerve stimulator for electronic pain block. *Science Advances* **2022**, *8* (40), No. eabp9169.
(125) Yang, Q.; Hu, Z.; Seo, M.-H.; Xu, Y.; Yan, Y.; Hsu, Y.-H.; Berkovich, J.; Lee, K.; Liu, T.-L.; McDonald, S.; Nie, H.; Oh, H.; Wu, M.; Kim, J.-T.; Miller, S. A.; Jia, Y.; Butun, S.; Bai, W.; Guo, H.; Choi, J.; Banks, A.; Ray, W. Z.; Kozorovitskiy, Y.; Becker, M. L.; Pet, M. A.;

https://doi.org/10.1021/acsaelm.3c00879
ACS Appl. Electron. Mater. XXXX, XXX, XXX−XXX

MacEwan, M. R.; Chang, J.-K.; Wang, H.; Huang, Y.; Rogers, J. A. High-speed, scanned laser structuring of multi-layered eco/bioresorbable materials for advanced electronic systems. *Nat. Commun.* **2022**, *13* (1), 6518.
(126) Yang, Q.; Liu, T.-L.; Xue, Y.; Wang, H.; Xu, Y.; Emon, B.; Wu, M.; Rountree, C.; Wei, T.; Kandela, I.; Haney, C. R.; Brikha, A.; Stepien, I.; Hornick, J.; Sponenburg, R. A.; Cheng, C.; Ladehoff, L.; Chen, Y.; Hu, Z.; Wu, C.; Han, M.; Torkelson, J. M.; Kozorovitskiy, Y.; Saif, M. T. A.; Huang, Y.; Chang, J.-K.; Rogers, J. A. Ecoresorbable and bioresorbable microelectromechanical systems. *Nature Electronics* **2022**, *5* (8), 526−538.
(127) Minev, I. R.; Musienko, P.; Hirsch, A.; Barraud, Q.; Wenger, N.; Moraud, E. M.; Gandar, J.; Capogrosso, M.; Milekovic, T.; Asboth, L.; Torres, R. F.; Vachicouras, N.; Liu, Q.; Pavlova, N.; Duis, S.; Larmagnac, A.; Vörös, J.; Micera, S.; Suo, Z.; Courtine, G.; Lacour, S. P. Electronic dura mater for long-term multimodal neural interfaces. *Science* **2015**, *347* (6218), 159−163.
(128) Ling, W.; Yu, J.; Ma, N.; Li, Y.; Wu, Z.; Liang, R.; Hao, Y.; Pan, H.; Liu, W.; Fu, B.; Wang, K.; Wang, H.; Li, L.; Sheng, X.; Peng, H.; Ning, B.; Yang, J.; Huang, X. Flexible Electronics and Materials for Synchronized Stimulation and Monitoring in Multi-Encephalic Regions. *Adv. Funct. Mater.* **2020**, *30* (32), 2002644.
(129) Phan, H.-P.; Zhong, Y.; Nguyen, T.-K.; Park, Y.; Dinh, T.; Song, E.; Vadivelu, R. K.; Masud, M. K.; Li, J.; Shiddiky, M. J. A.; Dao, D.; Yamauchi, Y.; Rogers, J. A.; Nguyen, N.-T. Long-Lived, Transferred Crystalline Silicon Carbide Nanomembranes for Implantable Flexible Electronics. *ACS Nano* **2019**, *13* (10), 11572−11581.
(130) Pham, T.-A.; Nguyen, T.-K.; Vadivelu, R. K.; Dinh, T.; Qamar, A.; Yadav, S.; Yamauchi, Y.; Rogers, J. A.; Nguyen, N.-T.; Phan, H.-P. A Versatile Sacrificial Layer for Transfer Printing of Wide Bandgap Materials for Implantable and Stretchable Bioelectronics. *Adv. Funct. Mater.* **2020**, *30* (43), 2004655.
(131) Truong, T.-A.; Nguyen, T. K.; Huang, X.; Ashok, A.; Yadav, S.; Park, Y.; Thai, M. T.; Nguyen, N.-K.; Fallahi, H.; Peng, S.; Dimitrijev, S.; Toh, Y.-C.; Yamauchi, Y.; Wang, C. H.; Lovell, N. H.; Rogers, J. A.; Do, T. N.; Nguyen, N.-T.; Zhao, H.; Phan, H.-P. Engineering Route for Stretchable, 3D Microarchitectures of Wide Bandgap Semiconductors for Biomedical Applications. *Adv. Funct. Mater.* **2023**, *33* (34), 2211781.
(132) Bose, S.; Volpatti, L. R.; Thiono, D.; Yesilyurt, V.; McGladrigan, C.; Tang, Y.; Facklam, A.; Wang, A.; Jhunjhunwala, S.; Veiseh, O.; Hollister-Lock, J.; Bhattacharya, C.; Weir, G. C.; Greiner, D. L.; Langer, R.; Anderson, D. G. A retrievable implant for the long-term encapsulation and survival of therapeutic xenogeneic cells. *Nature biomedical engineering* **2020**, *4* (8), 814−826.
(133) Garcia-Cortadella, R.; Schwesig, G.; Jeschke, C.; Illa, X.; Gray, A. L.; Savage, S.; Stamatidou, E.; Schiessl, I.; Masvidal-Codina, E.; Kostarelos, K.; Guimera-Brunet, A.; Sirota, A.; Garrido, J. A. Graphene active sensor arrays for long-term and wireless mapping of wide frequency band epicortical brain activity. *Nat. Commun.* **2021**, *12* (1), 211.
(134) Zhang, A.; Mandeville, E. T.; Xu, L.; Stary, C. M.; Lo, E. H.; Lieber, C. M. Ultraflexible endovascular probes for brain recording through micrometer-scale vasculature. *Science* **2023**, *381* (6655), 306−312.
(135) Luan, L.; Wei, X.; Zhao, Z.; Siegel, J. J.; Potnis, O.; Tuppen, C. A.; Lin, S.; Kazmi, S.; Fowler, R. A.; Holloway, S.; Dunn, A. K.; Chitwood, R. A.; Xie, C. Ultraflexible nanoelectronic probes form reliable, glial scar−free neural integration. *Science Advances* **2017**, *3* (2), No. e1601966.
(136) Galluccio, L.; Palazzo, S.; Santagati, G. E. Characterization of molecular communications among implantable biomedical neuro-inspired nanodevices. *Nano Communication Networks* **2013**, *4* (2), 53−64.
(137) Abita, J. L.; Schneider, W. Transdermal optical communications. *Johns Hopkins APL Technol. Dig.* **2004**, *25* (3), 261−268.
(138) Wang, G.; Liu, W.; Sivaprakasam, M.; Kendir, G. A. Design and analysis of an adaptive transcutaneous power telemetry for biomedical implants. *IEEE Transactions on Circuits and Systems I: Regular Papers* **2005**, *52* (10), 2109−2117.
(139) Ghovanloo, M.; Najafi, K. A wideband frequency-shift keying wireless link for inductively powered biomedical implants. *IEEE Transactions on Circuits and Systems I: Regular Papers* **2004**, *51* (12), 2374−2383.
(140) Bohorquez, J. L.; Chandrakasan, A. P.; Dawson, J. L. A 350 μW CMOS MSK Transmitter and 400 μW OOK Super-Regenerative Receiver for Medical Implant Communications. *IEEE Journal of Solid-State Circuits* **2009**, *44* (4), 1248−1259.
(141) Zeng, F. G.; Rebscher, S.; Harrison, W.; Sun, X.; Feng, H. Cochlear Implants: System Design, Integration, and Evaluation. *IEEE Reviews in Biomedical Engineering* **2008**, *1*, 115−142.
(142) Cho, N.; Yoo, J.; Song, S. J.; Lee, J.; Jeon, S.; Yoo, H. J. The Human Body Characteristics as a Signal Transmission Medium for Intrabody Communication. *IEEE Transactions on Microwave Theory and Techniques* **2007**, *55* (5), 1080−1086.
(143) Song, Y.; Hao, Q.; Zhang, K.; Wang, M.; Chu, Y.; Kang, B. The Simulation Method of the Galvanic Coupling Intrabody Communication With Different Signal Transmission Paths. *IEEE Transactions on Instrumentation and Measurement* **2011**, *60* (4), 1257−1266.
(144) Mazzilli, F.; Dehollain, C. 184 μW ultrasonic on−off keying/amplitude-shift keying demodulator for downlink communication in deep implanted medical devices. *Electron. Lett.* **2016**, *52* (7), 502−504.
(145) Zhang, Y.; Yang, C.; Chang, Z.; Li, Z.; Gao, H.; Luo, Y.; Xu, K.; Pan, G.; Zhao, B. An 8-Shaped Antenna-Based Battery-Free Neural-Recording System Featuring 3 cm Reading Range and 140 pJ/bit Energy Efficiency. *IEEE J. Solid-State Circuits* **2023**, *58* (11), 3194−3206.
(146) Teshome, A. K.; Kibret, B.; Lai, D. T. H. A Review of Implant Communication Technology in WBAN: Progress and Challenges. *IEEE Reviews in Biomedical Engineering* **2019**, *12*, 88−99.
(147) *ElectroMagnetic Compatibility (EMC) Standard for Radio Equipment and Services*; ETSI, 2019; pp 16−19.
(148) Vincent, C. A. Lithium batteries: a 50-year perspective, 1959−2009. *Solid State Ionics* **2000**, *134* (1), 159−167.
(149) Amar, A. B.; Kouki, A. B.; Cao, H. Power Approaches for Implantable Medical Devices. *Sensors* **2015**, *15* (11), 28889−28914.
(150) Agarwal, K.; Jegadeesan, R.; Guo, Y. X.; Thakor, N. V. Wireless Power Transfer Strategies for Implantable Bioelectronics. *IEEE Reviews in Biomedical Engineering* **2017**, *10*, 136−161.
(151) Nelson, B.; Karipott, S.; Wang, Y.; Ong, K. Wireless Technologies for Implantable Devices. *Sensors* **2020**, *20*, 4604.
(152) Pérez, P.; Veirano, F.; Silveira, F. A Compact Lithium-Ion Battery Charger for Low-Power Applications. *IEEE Transactions on Circuits and Systems II: Express Briefs* **2022**, *69* (3), 669−673.
(153) Wei, X.; Liu, J. Power sources and electrical recharging strategies for implantable medical devices. *Frontiers of Energy and Power Engineering in China* **2008**, *2* (1), 1−13.
(154) Mano, N.; Mao, F.; Heller, A. Characteristics of a Miniature Compartment-less Glucose−O2 Biofuel Cell and Its Operation in a Living Plant. *J. Am. Chem. Soc.* **2003**, *125* (21), 6588−6594.
(155) Sun, F.; Jiang, H.; Wang, H.; Zhong, Y.; Xu, Y.; Xing, Y.; Yu, M.; Feng, L.-W.; Tang, Z.; Liu, J.; Sun, H.; Wang, H.; Wang, G.; Zhu, M. Soft Fiber Electronics Based on Semiconducting Polymer. *Chem. Rev.* **2023**, *123* (8), 4693−4763.
(156) Lu, Y.; Yu, Z.-D.; Un, H.-I.; Yao, Z.-F.; You, H.-Y.; Jin, W.; Li, L.; Wang, Z.-Y.; Dong, B.-W.; Barlow, S.; Longhi, E.; Di, C.-a.; Zhu, D.; Wang, J.-Y.; Silva, C.; Marder, S. R.; Pei, J. Persistent Conjugated Backbone and Disordered Lamellar Packing Impart Polymers with Efficient n-Doping and High Conductivities. *Adv. Mater.* **2021**, *33* (2), 2005946.
(157) Li, N.; Yi, Z.; Ma, Y.; Xie, F.; Huang, Y.; Tian, Y.; Dong, X.; Liu, Y.; Shao, X.; Li, Y.; Jin, L.; Liu, J.; Xu, Z.; Yang, B.; Zhang, H. Direct powering a real cardiac pacemaker by natural energy of a heartbeat. *ACS Nano* **2019**, *13* (3), 2822−2830.

https://doi.org/10.1021/acsaelm.3c00879
ACS Appl. Electron. Mater. XXXX, XXX, XXX−XXX

(158) Tashiro, R.; Kabei, N.; Katayama, K.; Ishizuka, Y.; Tsuboi, F.; Tsuchiya, K. Development of an electrostatic generator that harnesses the motion of a living body: use of a resonant phenomenon. *JSME International Journal Series C Mechanical Systems, Machine Elements and Manufacturing* **2000**, *43* (4), 916.
(159) Tashiro, R.; Kabei, N.; Katayama, K.; Tsuboi, E.; Tsuchiya, K. Development of an electrostatic generator for a cardiac pacemaker that harnesses the ventricular wall motion. *Journal of Artificial Organs* **2002**, *5* (4), 239−245.
(160) Miao, P.; Mitcheson, P. D.; Holmes, A. S.; Yeatman, E. M.; Green, T. C.; Stark, B. H. Mems inertial power generators for biomedical applications. *Microsystem Technologies* **2006**, *12* (10), 1079−1083.
(161) Irani, A.; Bianco, M.; Tran, D.; Deyoung, P. D.; Wyld, M. L. R.; Li, T. H. Energy generating systems for implanted medical devices. Canadian Patent CA2689413A1, 2009.
(162) Nasiri, A.; Zabalawi, S. A.; Jeutter, D. C. A Linear Permanent Magnet Generator for Powering Implanted Electronic Devices. *IEEE Transactions on Power Electronics* **2011**, *26* (1), 192−199.
(163) Li, P.; Bashirullah, R. A Wireless Power Interface for Rechargeable Battery Operated Medical Implants. *IEEE Transactions on Circuits and Systems II: Express Briefs* **2007**, *54* (10), 912−916.
(164) Catrysse, M.; Hermans, B.; Puers, R. An inductive power system with integrated bi-directional data-transmission. *Sensors and Actuators A: Physical* **2004**, *115* (2), 221−229.
(165) Ghovanloo, M.; Najafi, K. A Wireless Implantable Multichannel Microstimulating System-on-a-Chip With Modular Architecture. *IEEE Transactions on Neural Systems and Rehabilitation Engineering* **2007**, *15* (3), 449−457.
(166) Lenaerts, B.; Puers, R. An inductive power link for a wireless endoscope. *Biosens. Bioelectron.* **2007**, *22* (7), 1390−1395.
(167) Ma, A.; Poon, A. S. Y. Midfield Wireless Power Transfer for Bioelectronics. *IEEE Circuits and Systems Magazine* **2015**, *15* (2), 54−60.
(168) Bercich, R. A.; Duffy, D. R.; Irazoqui, P. P. Far-Field RF Powering of Implantable Devices: Safety Considerations. *IEEE Transactions on Biomedical Engineering* **2013**, *60* (8), 2107−2112.
(169) Goto, K.; Nakagawa, T.; Nakamura, O.; Kawata, S. An implantable power supply with an optically rechargeable lithium battery. *IEEE Transactions on Biomedical Engineering* **2001**, *48* (7), 830−833.
(170) Cochran, G. V. B.; Kadaba, M. P.; Palmieri, V. R. External ultrasound can generate microampere direct currents in vivo from implanted piezoelectric materials. *Journal of Orthopaedic Research* **1988**, *6* (1), 145−147.

https://doi.org/10.1021/acsaelm.3c00879
ACS Appl. Electron. Mater. XXXX, XXX, XXX−XXX